Chapter one

Introduction

1.Introduction:

The goal of edge detection is to produce something like a line drawing of an image. In practice we will look for places in the image where the intensity changes quickly. Observe that, in general, the boundaries of objects tend to produce suddent changes in the image intensity. For example, different objects are usually different colors or hues and this causes the image intensity to change as we move from one object to another. In addition, different surfaces of an object receive different amounts of light, which again produces intensity changes. Thus, much of the geometric information that would be conveyed in a line drawing is captured by the intensity changes in an image. Unfortunately, there are also a large number of intensity changes that are not due to geometry, such as surface markings, texture, and specular reflections. Moreover there are sometimes surface boundaries that do not produce very strong intensity changes. Therefore the intensity boundary information that we extract from an image will tend to indicate object boundaries, but not always. Edges are boundaries between different textures. Edge also can be defined as discontinuities in image intensity from one pixel to another. The edges for an image are always the important characteristics that offer an indication for a higher frequency. Detection of edges for an image may help for image segmentation, data compression, and also help for well matching, such as image reconstruction and so on. Variables involved in the selection of an edge detection operator include Edge orientation, Noise environment and Edge structure. The geometry of the operator determines a characteristic direction in which it is most sensitive to edges. Operators can be optimized to look for horizontal, vertical, or diagonal edges. Edge detection is difficult in noisy images, since both the noise

and the edges contain high-frequency content. Attempts to reduce the noise result in blurred and distorted edges. Operators used on noisy images are typically larger in scope, so they can average enough data to discount localized noisy pixels. This results in less accurate localization of the detected edges. Not all edges involve a step change in intensity. Effects such as refraction or poor focus can result in objects with boundaries defined by a gradual change in intensity. The operator needs to be chosen to be responsive to such gradual change in those cases. So, there are problems of false edge detection, missing true edges, edge localization, high computational time and problems due to noise etc. Therefore, the objective is Enhancement of Edge Detection of Thyroid Scintigraphy Using Image Processing Technique.

(Gonzalez, 2009).

1.2. Problem of study:

In imaging test the image taken from patient were coarse and diffuse or with unsharpness, blurring that will lead to difficulties in diagnosis of thyroid cancer or other disorder need imaging and may be lead to wrong diagnosis that is enough reason to draw attention to this issue.

1.3. Objectives of the study:

1.3.1. General objectives of the study:

The main objective of this study is Enhancement of Edge Detection of Thyroid Scintigraphy Using Image Processing Technique.

1.3.2. Specific Objectives:

- Read image
- To detect region of interest
- To remove background
- to retain the image

1.4. Overview of the study:

This study falls into five chapters chapter one deal with introduction , chapter two deal with literature review that includes Thyroid Anatomy and Physiology, Nuclear Medicine Examination of thyroid, Image Processing in Nuclear Medicine, Matlab simulation and programming in thyroid and Previous studies , chapter three deal with materials and methods , chapter four deal with result of the study and chapter five deal with discussion, conclusion and recommendation.

Chapter two

literature Review

2.1 Thyroid Anatomy and Physiology:

2.1.1. Embryology and Anatomy:

The normal thyroid gland begins as a primitive diverticulum at the base of the tongue in the third week of gestation and grows caudally toward its ultimate position anterior to the thyroid cartilage. In the adult it forms a butterfly-shaped structure weighing about 20 grams. Some thyroid tissue may remain along the thyroglossal duct to form a pyramidal lobe or a thyroglossal thyroid remnant in post-natal life. In rare cases the thyroid fails to descend and forms at the base of the tongue (lingual thyroid) where it may present as a mass. The thyroid originates near the formation site of the aortic sac, and for this reason accessory thyroid tissue may be found in the mediastinum. (Williams , 2003).

The normal thyroid is made up predominantly of follicular cells whose function is the production, storage and secretion of thyroid hormone. These cells are able to trap iodine and produce thyroxine by about the 11th week of gestation. The follicular cells, possibly under the influence of TSH, arrange themselves to form follicles into which they secrete thyroglobulin. A second population of cells, known as parafollicular or C cells, is derived from the neural crest. These appear about midgestation and are responsible for the secretion of calcitonin. The C cells do not form follicles and their secretory polarity is oriented toward the capillaries.

There are relatively few lymphatics in the thyroid compared to capillaries and these are concentrated in the pericapsular areas. Thyroidal lymphatics drain to nodes on the thyroid, trachea, larynx and in the tracheo-esophageal groove as well

as to the deep cervical nodes along the internal jugular vein. Drainage to nodes in the upper mediastinum is also common (Fig. 1). (Williams , 2003).

2.1.2 .Normal Physiology and Metabolism :

The follicular cells reversibly take up iodide ions from the bloodstream against a 30-fold concentration gradient and irreversibly convert them to an organic form, which is secreted into the follicles (Fig. 2.1). The steps of uptake and organification are stimulated by thyroid stimulating hormone (TSH). Uptake is competitively inhibited by large anions such as thiocyanate and perchlorate. Organification is blocked by the thyroid-blocking drugs, propylthiouracil (PTU) and methimazole. Oxidized iodine is secreted into the colloid where synthesis of mono- and diiodotyrosines occurs, going on to the production of thyroxine (T4) and triiodothyronine (T3). These steps are also blocked by anti-thyroid drugs. Within the follicle, thyroid hormones are bound to thyroglobulin (Tg). The storage capacity of the thyroid as an endocrine gland is exceptional: an average gland contains about 3 (Williams, 2003).
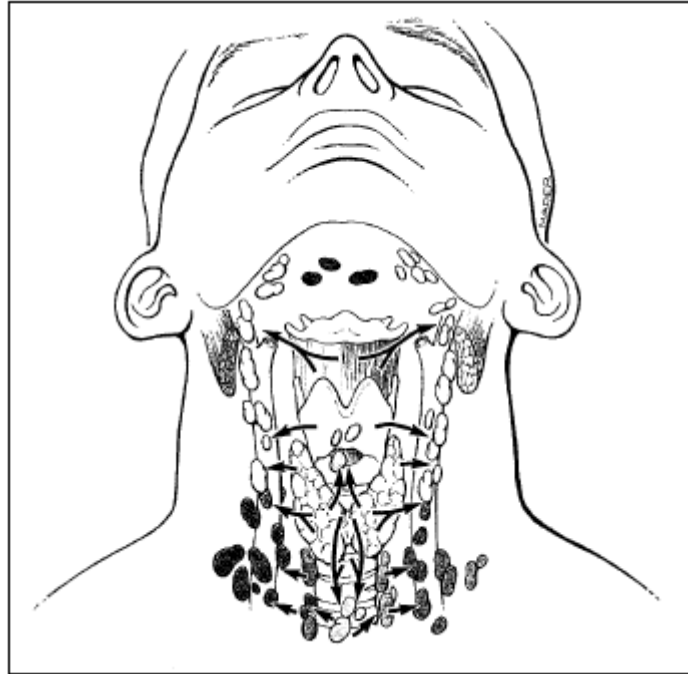
Figure 2.1. Anatomic distribution of lymph nodes that drain the thyroid gland. (Williams, 1991).

month's supply of hormone. The amount of iodine contained in a normal gland, subject to an adequate iodine intake, is about 7-10mg. Release of hormone from the follicle is stimulated by TSH and inhibited by iodide and lithium.

Tg is a large protein (660kd) that serves as the matrix for thyroid hormone synthesis in the follicles and also as the storage vehicle. Tg synthesis is stimulated by TSH via the cyclic AMP mechanism. Of the 134 tyrosine residues in the molecule, no more than 15-17 are usually iodinated, including no more than 2-4 molecules of T4 and T3. The release of the hormone seems to result in the destruction of the Tg molecule, seemingly an inefficient process when the energy costs of synthesizing such a large molecule are considered. Normally, Tg is largely retained within the follicles, but it may be released into the blood stream in disease states. Tg is often produced by neoplasm derived from follicular cells and is a useful marker for recurrence of tumor. Production of thyroid hormone is regulated by the pituitary gland through the secretion of TSH, which in turn is regulated by hypothalamic production of thyrotropin-releasing hormone (TRH).
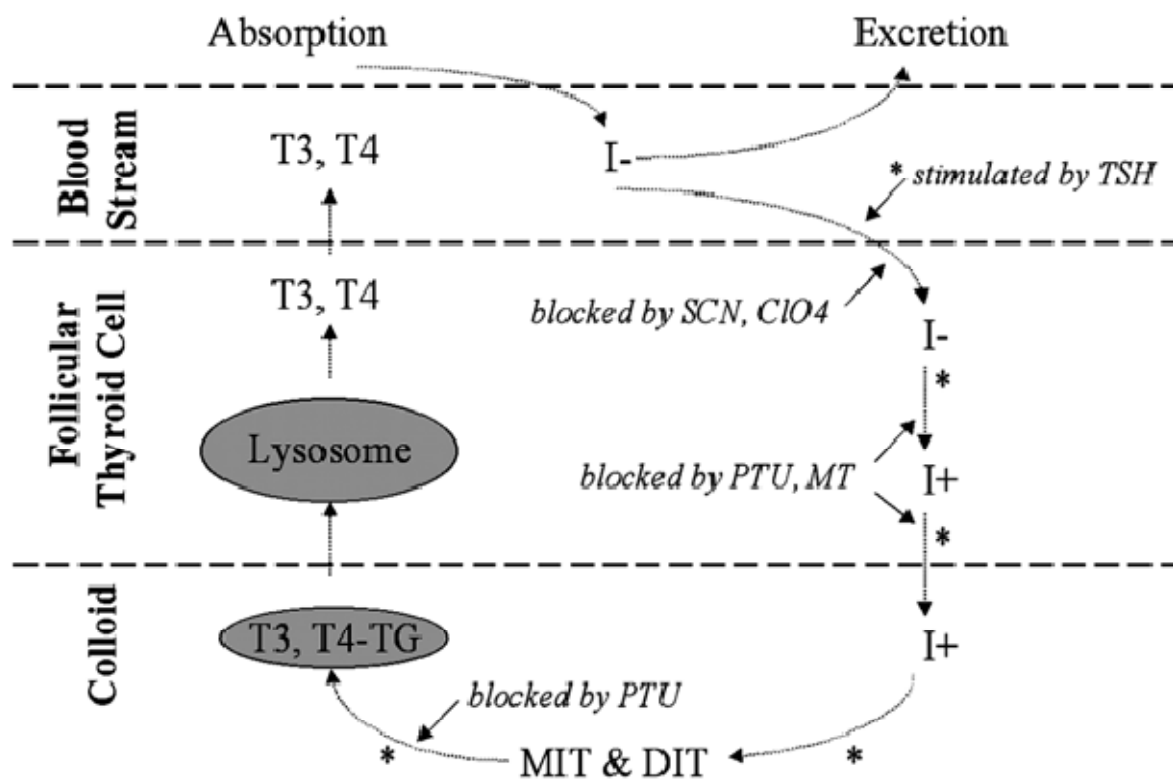
Figure 2.2 A schematic representation of iodine metabolism in the thyroid gland. SCN-thiocyanate; ClO4-perchlorate; PTU-propylthiouracil; MT-methimazole; MIT&DIT-mono- and di-iodo-tyrosine; Tg-thyroglobulin; *-sites stimulated by TSH (Williams, 1991).
.

TRH is a tripeptide that may be transported to the pituitary along direct neuronal interconnections. Circulating levels of thyroid hormone, especially T3, provide the negative feedback required to regulate the level of TRH and TSH.

Circulating thyroid hormone is protein-bound. Thyroxine-binding proteins are present in the fetal blood stream by mid-gestation, an important consideration in Nuclear Medicine as maternal exposure to iodine isotopes will be associated with fetal uptake and retention through this mechanism.

Calcitonin, the secretory product of the C cells, is a polypeptide of 32 amino

acids, whose major effect is to inhibit osteoclastic bone resorption. In humans the physiological importance of calcitonin remains unclear. Thyroidectomized patients with normal parathyroid gland function do not exhibit any apparent abnormality of bone metabolism. (Williams, 2003).

2.2. Nuclear Medicine Examination of thyroid:

Radionuclide imaging and the measurement of thyroid radioactive iodine uptake (RAIU) both play an important role in the investigation of patients with thyroid disorders, especially those with thyroid nodules. (A.P. Witkin, 1983).

2.2.1. Thyroid Scintigraphy:

With the development of fine needle aspiration biopsy (FNA) for evaluation of nodular disease combined with the exquisite anatomic detail provided by sonography, CT, and MRI, the use of thyroid scintigraphy has decreased appropriately. However, itwill continue to play an important role in the functional evaluation of a variety of thyroid disorders aswell as the detection of metastatic thyroid cancer. Technetium-99m pertechnetate is the most readily available radionuclide employed for thyroid imaging. Pertechnetate ions (TcO^-_4) are trapped by the thyroid in the same manner as iodine through an active iodine transporter, but pertechnetate ions are not organified. 123Iodine is both trapped and organified by the thyroid gland, allowing overall assessment of thyroid function. Since 123I is cyclotron-produced and has a relatively short half-life of 13.6 hours, it is more expensive and advance notice is necessary for imaging. Because of its inferior image quality and the high thyroid and total body radiation dose from its β-emission, 131I is not used for routine thyroid imaging other than for metastatic thyroid cancer assessment. Due primarily to less background activity, 123I imaging provides somewhat higher quality images than 99mTc, but the diagnostic

information provided by each is roughly equivalent . 123I imaging is used in specific situations, suchas retrosternal goiter.

The normal thyroid scintigram is shown in Figure 2.3 High-resolution images are obtained by using a pinhole collimator, thus permitting the detection of nodules as small as 5mmin diameter. The oblique views permit detection of small nodules obscured by overlying or underlying physiological activity. Pinhole SPECT has been used to better detect subtle abnormalities. The radionuclide is distributed homogeneously throughout the gland with some increase seen centrally due to physiological thickness of the gland there; activity within the isthmus is variable and must be
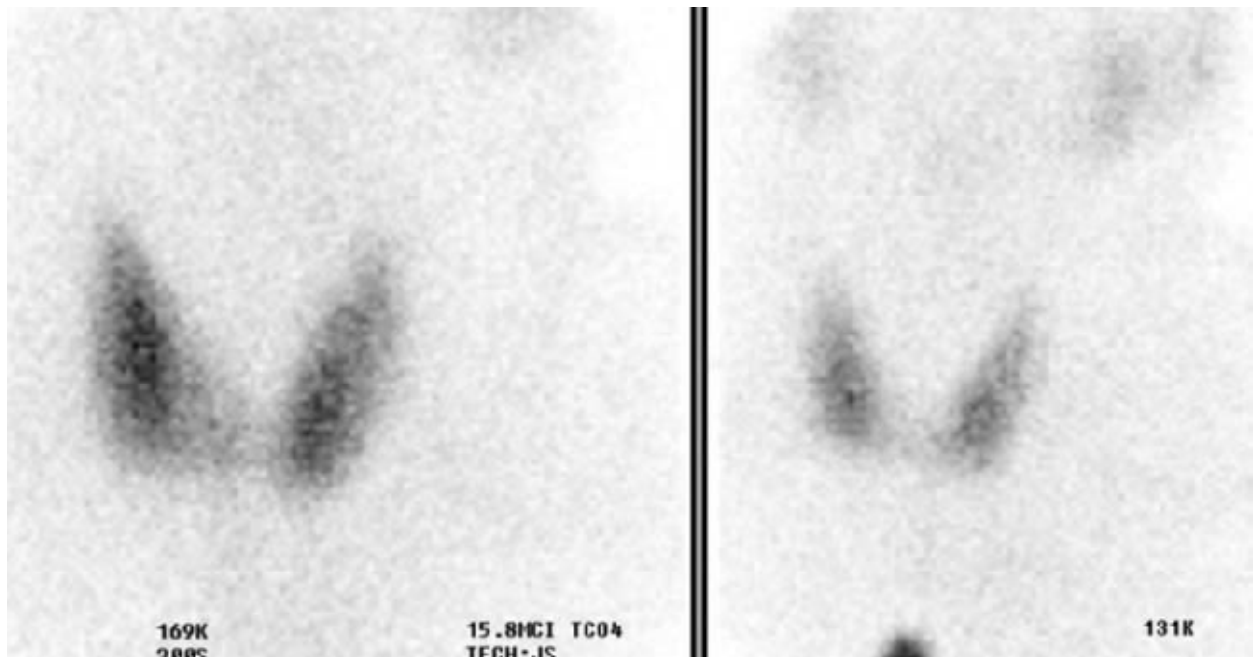

Figure 2.3 Normal 99mTc thyroid scan. Symmetric, homogeneous uptake with less intense salivary gland uptake and only mild background uptake. The inferior activity is due to a 57Co marker at the suprasternal notch (Peter F, 2005).

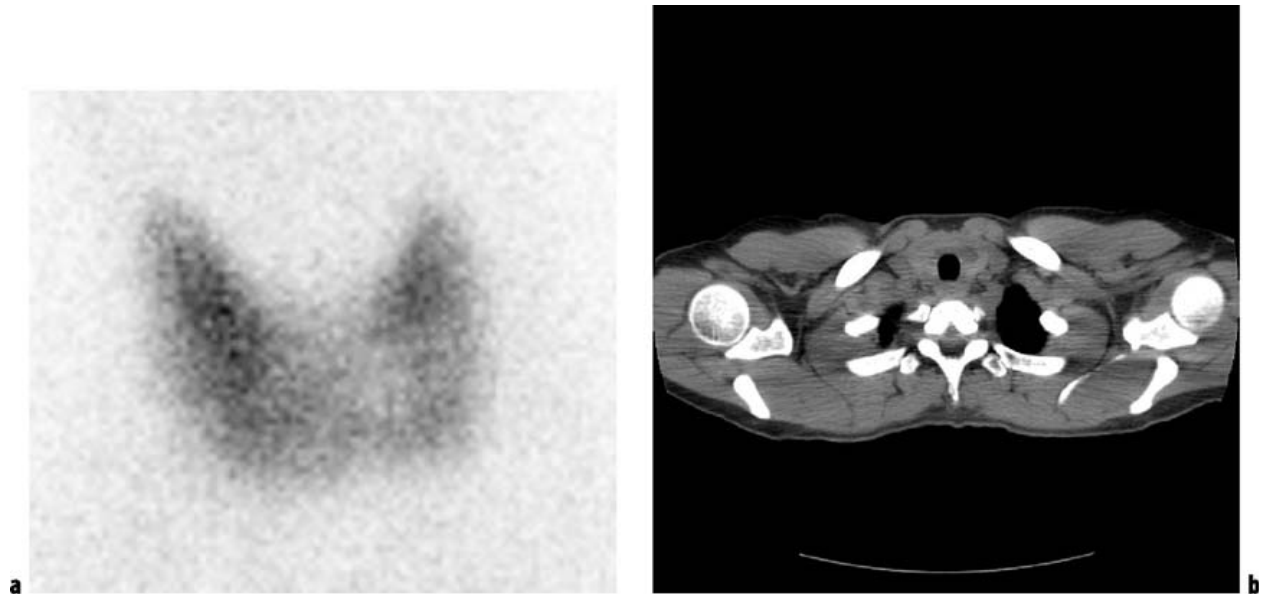**Figure 2.4** Subtle cold nodule. 99mTc pertechnetate anterior view**a**demonstrates a subtlehypofunctioning left lower pole nodule extending into the isthmus, confirmed on a subsequent contrast-enhanced CT **b** to be a thyroid cyst (Peter F, 2005).
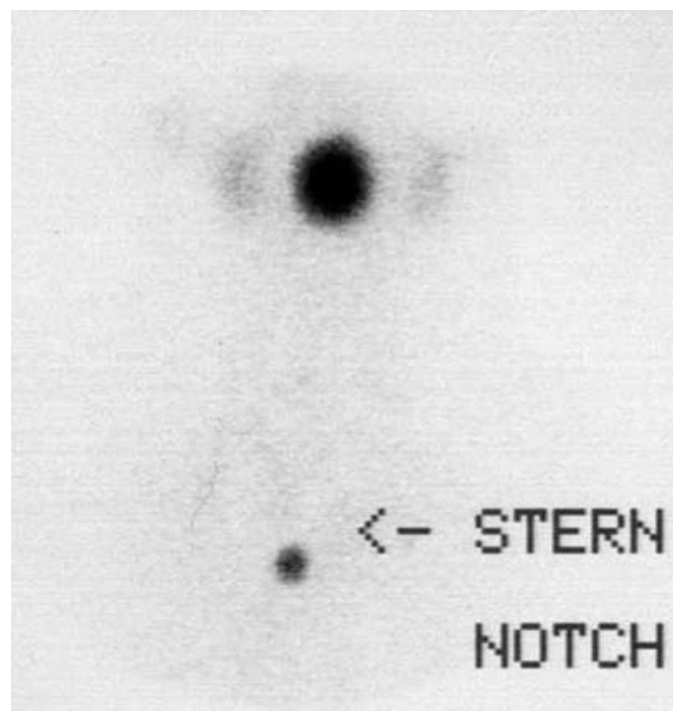

Figure2.5. Lingual ectopic thyroid. An anterior 99mTc pertechnetate image demonstrates a focus of activity at the base of the tongue in this neonate. (Peter F, 2005).

correlated with physical examination and/or other imaging (Figure 2.3). With pertechnetate, salivary glands, gastric mucosa, esophagus, and blood pool background are seen in addition to thyroid activity. Due to delayed imaging, salivary gland activity is often absent with 123I imaging. In the euthyroid gland, thyroid activity should be greater than that of the salivary glands. Anatomic variations are relatively frequent and may include agenesis, hemiagenesis, and ectopia (Figure 2.5) as well as mere asymmetry. Ectopia is typically associated with hypothyroidism. Significant concavity of the lateral margin should be considered suspicious of a hypofunctioning nodule, and exaggerated convexity is often seen with diffuse goiters. The pyramidal lobe, a remnant of the distal thyroglossal duct, is identified in less than 10% of euthyroid patients, but is visualized in as many as 43% of patients with Graves' disease (Figure 2.6). Extrathyroidal accumulation of the radiopharmaceutical usually represents ectopic thyroid tissue or metastatic thyroid carcinoma if gastroesophageal and salivary gland activity can be excluded (Peter F, 2005).

2.2.2. Multinodular Goiter:

The patient with multinodular goiter (MNG) may present with what seems to be a solitary thyroid nodule, diffuse enlargement of the gland, or hyperthyroidism. Development of MNG is related to cycling periods of stimulation followed by involution and may be idiopathic or occur as a result of endemic iodine deficiency. Over time the gland enlarges and evolves into an admixture of fibrosis, functional nodules, and non-functioning involuted nodules. Scintigraphically, the MNG
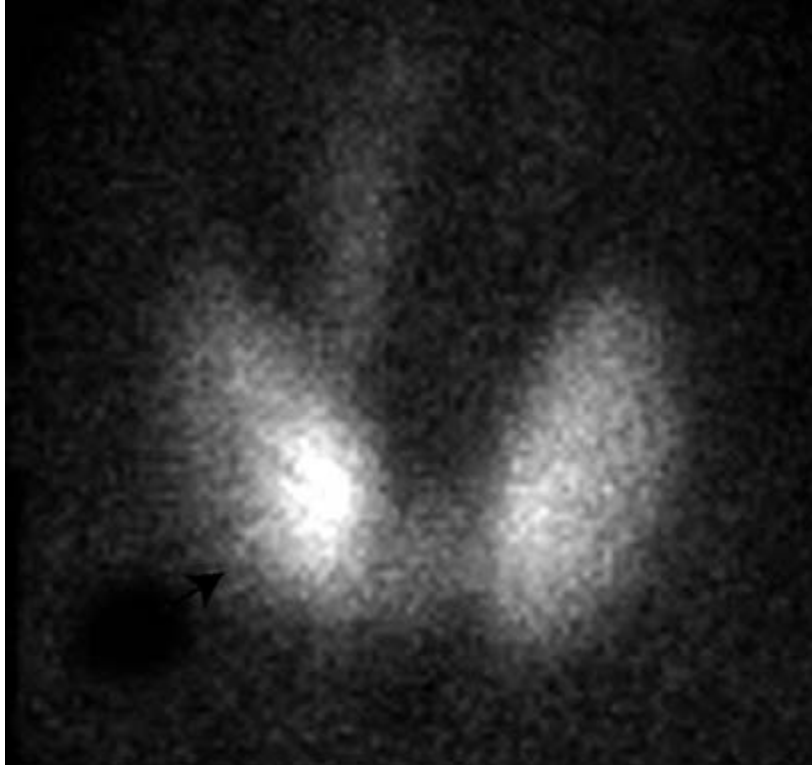
Figure2.6. Graves' disease. 99mTc thyroid scan shows a pyramidal lobe emanating from the medial aspect of the right lobe. Note the convex contour of the gland and the diminished background activity (Peter F, 2005).

is a heterogeneously-appearing, asymmetrically enlarged gland withmultiple cold, warm, and hot areas of various sizes (Figure 2.7). The incidence of thyroid carcinoma in MNG is low at 1–6%, but a dominant or enlarging cold nodule should be
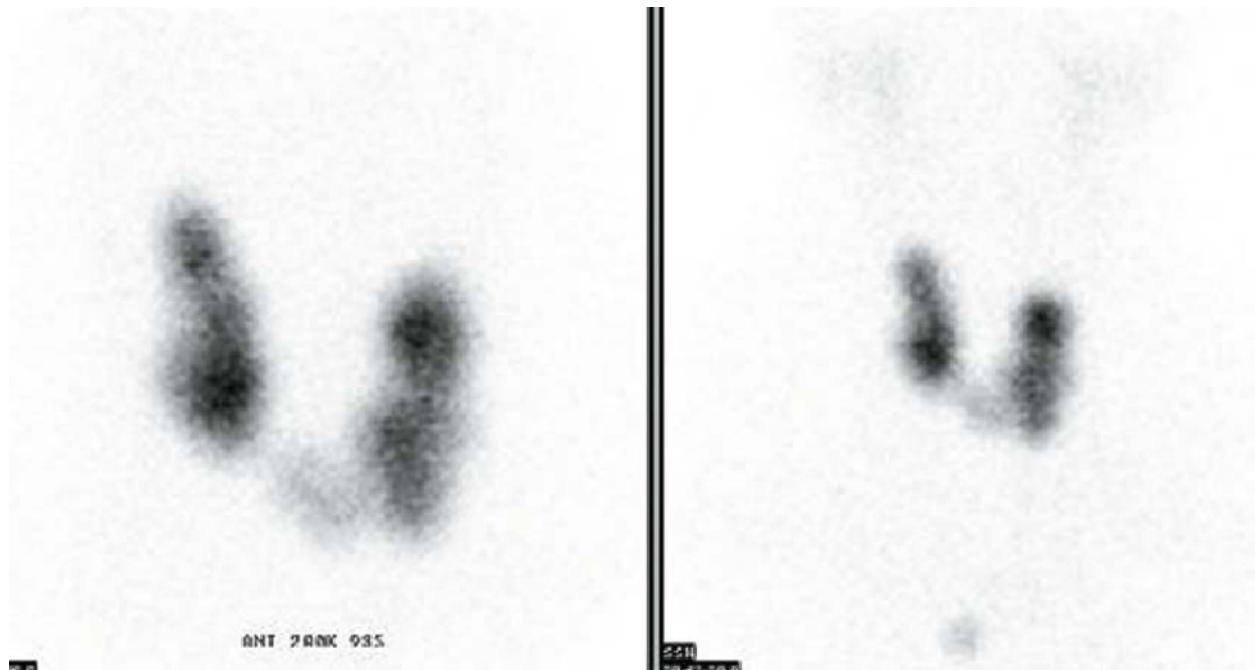
Figure 2.7. Multinodular goiter. An anterior 99mTc pertechnetate view demonstrates asymmetric enlargement of the gland with multiple areas of increased, decreased, and normal activity. The decreased background activity and faint salivary gland activity is compatible with the clinical impression of toxic multinodular goiter (Peter F, 2005).

biopsied. The differential diagnosis includes autoimmune Hashimoto's thyroiditis, multiple adenomas, and multifocal carcinoma. Further characterization of the gland with ultrasound, CT, or MRI does not appreciably aid clinical diagnosis (Peter F, 2005) .

2.2.3. Thyroid Nodules:

The management of patients with a solitary thyroid nodule remains controversial, related to the high incidence of nodules, the infrequency of thyroid malignancy, and the relatively low morbidity and mortality associated with differentiated thyroid cancer (DTC) . Thyroid nodules may contain normal thyroid tissue, benign hypofunctioning tissue (solid, cystic, or complex), hyperplastic or autonomously functioning benign tissue, or malignant neoplasm. The evaluation of the patient with a solitary thyroid nodule is directed towards differentiating benign

frommalignant etiologies. Autopsy series have demonstrated a 50% incidence of single or multiple thyroid nodule(s), only 4% of which are malignant. Ultrasonography detects single or multiple thyroid nodules in 40% of patients with no known thyroid disease. The incidence of thyroid nodules increases with advancing age, and is more frequent in females and in patients with a prior history of neck or facial irradiation. Hypofunctioning ("cold") nodules concentrate less radioisotope relative to the remainder of the thyroid gland (see Figure 2.4). Eighty-five to ninety percent of thyroid nodules are hypofunctioning, but only 10–20% of cold nodules are malignant . The remaining hypofunctioning nodules consist of degenerative nodules, nodular hemorrhage, cysts, thyroiditis, infiltrative disorders such as amyloid, and non-thyroid neoplasm. Clinical features that suggest thyroid cancer include male gender, a prior history of radiation exposure up to 15 Gy (1500 rad), a family history of medullary or papillary thyroid carcinoma, and relative youth. Local fixation of the noduleor palpable adenopathy is also suggestive. Recentrapid enlargement of a nodule is more often related to hemorrhage into a cyst or nodule rather than carcinoma. (Bankman, 2000).

Although ultrasound and MRI are sensitive for the detection of thyroid nodules, specificity for malignancy is poor. Similarly, sensitivity for detectionof thyroid cancer is approximately 90% with scintigraphy, but specificity is poor at 15–20%. If extrathyroidal activity is seen in the neck on thyroid scintigraphy in a patient with a solitary thyroid nodule, metastatic thyroid carcinoma is likely. Some investigators have recommended the use of serum thyroglobulin and calcitonin determinations to improve the accuracy of clinical assessment and scintigraphy.

A hot or warm(hyperfunctioning) nodule concentrates the radioisotope to a greater degree than the normal thyroid gland and represents 10–25% of palpable nodules in patients. In over 99% of cases, a hot thyroid nodule is benign and biopsy is unnecessary. Although a functioning thyroid nodule in the euthyroid patient may

represent hyperplastic (sensitive to TSH stimulation) tissue, most are autonomously functioning thyroid nodules (AFTN) arising independently of TSH stimulation. Biochemical hyperthyroidism, often subclinical, is present in 74% of patients at presentation, although overt hyperthyroidism is less common. Over a period of 3 years after detection, 33% of AFTNs enlarge in patients not receiving definitive therapy, and 24% of euthyroid patients develop hyperthyroidism . In euthyroid patients, surrounding extranodular thyroid tissue will be visible (Figure 2.8a), thyroid function studies will be normal, and these patients can be followed on an annual basis. If hyperthyroidism
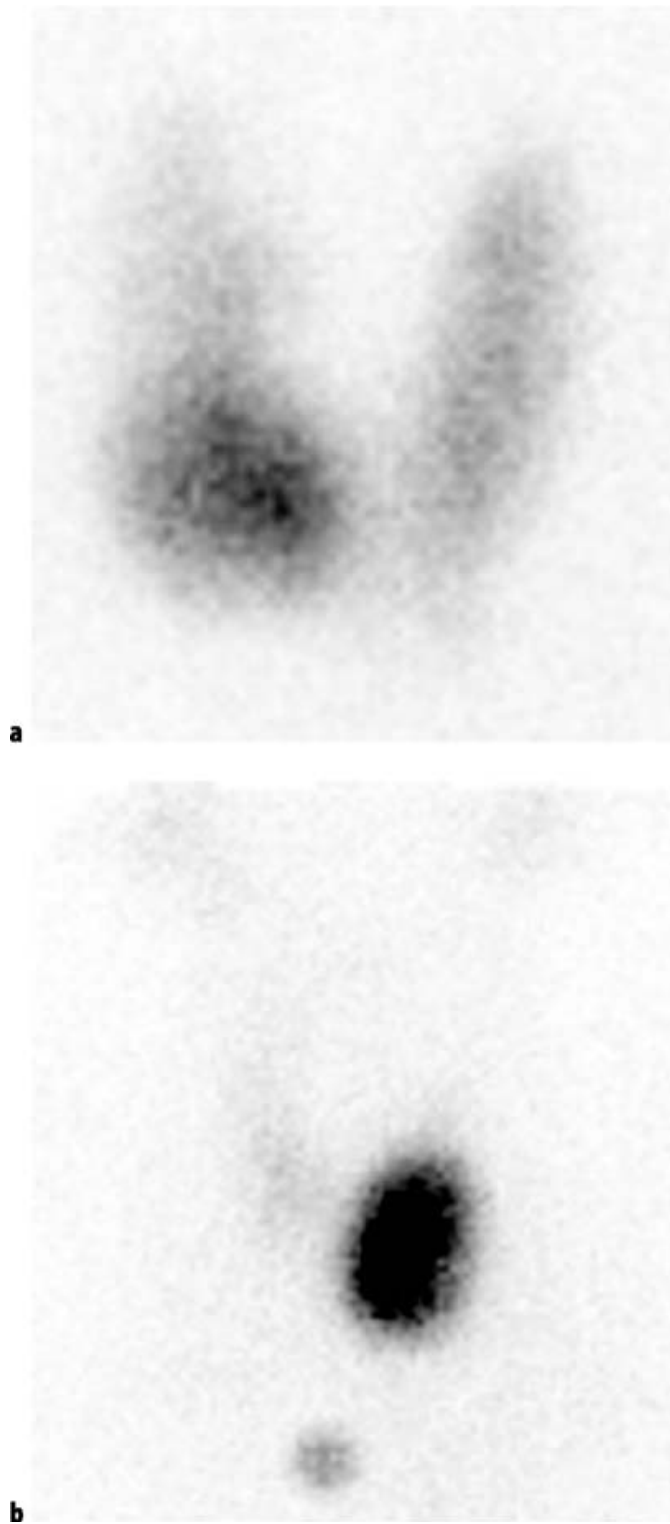
Figure 2.8. Autonomously functioning thyroid nodule. a An anterior 99mTc thyroid image reveals a focus of increased uptake in the lower pole of the right lobe consistent with a hyperfunctioning nodule. b A focus of markedly increased activity in the lower pole of the left lobe accompanied by virtual complete

suppression of extranodular activity and decreased background and salivary gland activity is consistent with toxic adenoma, subsequently confirmed by an undetectable serum TSH (Peter F, 2005).

exists, the surrounding normal thyroid tissue will be suppressed, and the TSH level will be undetectable (Figure 2.8b). Spontaneous cystic degeneration occurs in 27%, manifested by central photopenia; there is little concern for malignancy. Discordant thyroid imaging is a dissociation between trapping and organification, measured respectively with 99mTc pertechnetate and 123I. It occurs in only 2–8% of thyroid nodules and is not specific for malignant disease. A nodule that traps 99mTc (hot) but is unable to organify iodine (cold) is much more likely to be benign than malignant. If it is assumed that8%of hot noduleswith 99mTc are cold with 123I, and if 10% of those are malignant, then less than 1% of hot nodules seen with 99mTc imaging are malignant. Additional radioiodine imaging of hot nodules identified on a 99mTc scan should probably be reserved for patients deemed at higher risk for malignancy (Peter F, 2005).

2.2.4. Hyperthyroidism

Hyperthyroidism is a clinical syndrome of tachycardia, weight loss, and hypermetabolism resulting from supraphysiological circulating levels of thyroid hormones, leading to suppression of TSH secretion. Most cases of hyperthyroidism are due to increased endogenous synthesis and secretion of thyroid hormones from the thyroid.Clinical assessment combined with circulating hormone and thyroid autoantibody measurements, thyroid scintigraphy, and RAIU usually al- low identification of the various disease processes that may be responsible. Graves' disease (autoimmune diffuse toxic goiter) is due to the presence of thyroid-stimulating immunoglobulins and is associated with autoimmune exophthalmos and pretibialmyxedema. Although it occurs primarily in young women, it may also

occur in children and in the elderly. Radioiodine uptake will usually be elevated at 4 hours and/or 24 hours, and the gland will reveal diffuse enlargement in most cases with increased thyroid activity and minimal background and salivary gland activity (Figure 2.6). Hyperplasia of the pyramidal remnant is seen as increased paramedial activity in as many as 43% of Graves' patients. Occasionally, the gland will appear normal size. The low RAIU (usually ≤5%) of hyperthyroid patients with subacute thyroiditis, postpartum thyroiditis, silent thyroiditis, and surreptitious thyroid hormone administration is easily differentiated from the normal RAIU . Although ultrasound demonstrates an enlarged homogeneously hypoechoic gland with prominent vascularity on color-flowDoppler imaging ("thyroid inferno"), it is usually unnecessary for diagnosis clinically. The thyroid scan should easily be able to distinguish toxic nodular goiters from Graves' disease. The clinical importance of this is that many patients with toxic nodular goiter will require a higher dose of 131I for therapy than will Graves' disease patients (Peter F, 2005).

2.2.4.1 Radioiodine Therapy of Hyperthyroidism:

Graves' disease and toxic nodular goiter may be treated successfully with 131I therapy. Radioiodine was first used for the treatment of hyperthyroidism in 1941 and has since evolved to the treatment modality of choice for the majority of adult patients, particularly in the USA. Antithyroid drug therapy achieves a permanent remission in only 10–40% of patients, but is used initially in many patients, particularly in Europe and Asia. Although subtotal thyroidectomy is effective and complications are infrequent, thyroidectomy is used only occasionally at present. It is normally limited to patients in whom radioiodine is unsuitable, such as women whomay be pregnant, or who have extremely large goiterswith compressive symptoms. Radioiodine therapy is effective, practical, inexpensive, and available

on an outpatient basis. Prior to initiation of therapy, the diagnosis of hyperthyroidism must be confirmed by elevation of thyroid hormone levels and suppression of circulating TSH.An elevated RAIU confirms that endogenous thyroidal secretion is the source of the hyperthyroidism and aids in excluding other etiologies ofhyperthyroidism, suchas silent thyroiditis, subacute thyroiditis, postpartum thyroiditis, iodine-induced hyperthyroidism, and factitious hyperthyroidism, all of which are associated with a low RAIU. Rarely, clinical hyperthyroidism with diffuse goiter and elevated RAIU may be related to excessive secretion of human chorionic gonadotropin (HCG) by a trophoblastic tumor or by inappropriate secretion of TSH by a functioning pituitary adenoma. The presence of exophthalmos, pretibialmyxedema, and diffuse goiter on physical examination confirms Graves' disease as the etiology. Otherwise, thyroid scintigraphy is useful to differentiate diffuse involvement due to Graves' disease from localized disease due to AFTN.

The patientmust be counseled prior to therapy regarding the advantages and disadvantages of alternative therapies. Because iodide readily crosses the placenta, 131I may not be administered during pregnancy so a pregnancy test is mandatory prior to administration. Exposure of the fetus to 131I after the 10th week of gestation may result in severe fetal hypothyroidism. The effectiveness of radioiodine treatment for hyperthyroidism is due to radiation-induced cellular damage resulting from high-energy beta emission, the magnitude of which is directly proportional to the radiation dose received by the thyroid gland. The major effect of radiation is impairment of the reproductive capacity of follicular cells. The radiation dose to the thyroid is related to (1) the amount of radioiodine administered, (2) the fraction deposited in the gland (uptake), (3) the duration of retention by the thyroid (biologic half-life), and (4) the radiosensitivity of the irradiated tissue. Administered dose is usually calculated with the goal of

administering approximately 70–120 Gy (7000–12 000 rad) to the thyroid gland . Some practitioners have adopted a fixed dose administration, usually approximately 370MBq(10mCi)with perhaps 300MBq(8mCi) for a small gland and 440–520MBq(12 to 14mCi) for a large gland. In the UK, a relatively larger fixed dose of 550 MBq (15 mCi) is given to the majority of adult patients. Other practitioners will calculate a dose of 3–4.4 MBq (80 to 120 µCi) per gram of thyroid tissue for the usual patient with Graves' disease. Even higher dosages of up to 7.4 MBq (200 µCi) per gram will be used to produce a more rapid response in patients with severe hyperthyroidism. The calculation is made as follows: administered microcuries = µCi/g desired × gland weight (g) × 100 ÷ percent uptake (24 hours). A higher dose may also be required for patients with toxic nodular goiter, in patients previously treated with antithyroid medications, patients with extremely large glands, patients with rapid iodine turnover (a 4 h/24 h RAIU ratio>1), and in patients with renal insufficiency. Although estimation of thyroid size is relatively accurate for glands weighing less than 60 grams, the degree of inaccuracy increases in larger glands. Ultrasound may provide an accurate estimation of size, but the increase in accuracy of thyroid radiation dose determination is limited (Peter F,2005).

The complications of radioiodine therapy include rare exacerbation of hyperthyroidism, possible exacerbation of existing Graves' orbitopathy, and post-therapeutic hypothyroidism. It is estimated that less than 10% of patients require retreatment, and this is rarely undertaken before 3–4 months following therapy. Most practitioners will give at least 20–30% more radioiodine on a second treatment.Pretreatmentwith antithyroid medications is advisable in elderly patients, in patients with known cardiac disease, and in patients with large thyroid glands, particularlymultinodular goiters. These medications should be discontinued 48–72 hours prior to administration of 131I, and it is preferable to wait several days

before reinitiation of therapy. The administration of beta blockers before or after therapy serves only to ameliorate peripheral manifestations of hyperthyroidism and will not affect therapeutic efficacy of radioiodine. The incidence of early post-131Ihypothyroidism varies from 10% to 50% according to the dose administered. Subsequently, there is an additional incidence of hypothyroidism at a relatively constant rate of 2–3% per year. A similar incidence of hypothyroidism occurs following surgery. Some degree of hypothyroidism may be a natural consequence of the autoimmune process of Graves' disease, since a small percentage of patients treated only with antithyroid medications will become hypothyroid during long-termfollow-up after remission (Peter F,2005).

Although radiation exposure of more than 500 mGy (50 rad) is reported to increase theoccurrence of leukemia, with a peak incidence at approximately 6 years after exposure, a single 131I treatment delivers only 80–160 mGy (8–16 rad) to the blood and has not been associated with any increased incidence of leukemia, thyroid cancer, infertility, or congenital malformations. Although the desire for subsequent pregnancy is not a contraindication to radioiodine therapy for hyperthyroidism, patients are usually advised to avoid conception for 6 months in case retreatment is required (Peter F, 2005).

Following radioiodine therapy, the patient should be advised to have serumthyroid hormone and TSH levels checked within 2 to 3 months. Patients may be symptomatically improved within 4 to 6 weeks, but clinically significant hypothyroidism rarely occurs before 2 to 3 months. Hypothyroidism is only a problem if not adequately treated, and many practitioners will initiate thyroxine replacement therapy at the earliest indication of post-therapy hypothyroidism.

2.2.5. Thyroiditis:

Thyroiditis may be classified as acute, subacute, chronic/autoimmune, and other miscellaneous types; these different types of thyroiditis are unrelated to each other. Acute suppurative thyroiditis is rare and is caused by hematogenous spread of infectious organisms.This is usually defined clinically and evaluated by
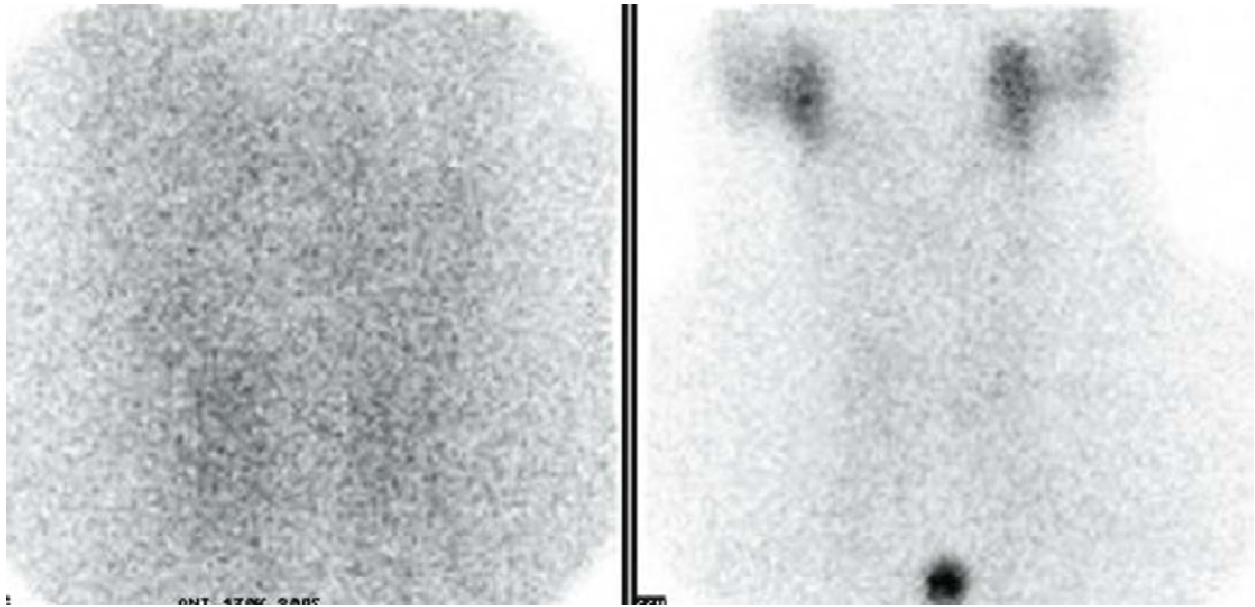
Figure 2.9. Subacute thyroiditis. An anterior 99mTc image reveals markedly reduced activity in the thyroid bed as compared to background and salivary glands (Peter F, 2005).

CT and/or sonography; scintigraphy is only rarely performed. Subacute (de Quervain's) thyroiditis is a benign, self-limited transient inflammatory disease of the thyroid, presumed to be of viral etiology. It may affect the gland diffusely or focally and usually presents as a tender gland in a patient with mild systemic symptoms and anelevated erythrocyte sedimentation rate. Serum thyroglobulin (Tg) is elevated and antithyroid antibodies are only marginally increased. A shortliveddestruction-induced thyrotoxicosis is followed by several months of hypothyroidism, usually subclinical. Thyroid scintigraphy will show poor thyroid visualization with increased background activity and an RAIU of <5% (Figure

2.9). Most patients are eventually left with a normal thyroid gland, both histologically andfunctionally. Symptoms respond to non-steroidal or steroidal anti-inflammatory agents and beta blockade. A second variety of thyrotoxic subacute thyroiditis is termed silent lymphocytic thyroiditis and is similar in presentation to de Quervain's thyroiditis except for the absence of pain, tenderness, and prodromal systemic symptoms. The etiology is thought to be an exacerbation of underlying autoimmune thyroid disease. Thyroid autoantibodies are present in high titers, but often diminish as the thyrotoxic phase resolves. A destruction-induced hyperthyroidismis accompanied by markedly suppressed RAIU and mild thyromegaly, all of which resolve over months. This entity presents more frequently in postpartum women (termed postpartum thyroiditis) and tends to recur with subsequent pregnancies. Many of these women will eventually develop permanent hypothyroidism. Chronic Hashimoto's autoimmune lymphocytic thyroiditis is the most common cause of hypothyroidism in the Western world and usually presents in women with a small to moderatelyenlarged firm goiter, elevated antithyroglobulin and/or antimicrosomal (antiperoxidase) antibodies, and rarely any tenderness. Patients may be euthyroid or hypothyroid and rarely hyperthyroid. Scintigraphy reveals inhomogeneous activity throughout the gland in 50%, though a pattern of multinodular goiter, solitary hot nodule, or solitary cold nodule as well as a normal scan may occur. RAIU may be normal, low, or elevated. Biopsy is rarely necessary for diagnosis, and most patients are treated with thyroid hormone supplementation. Iodine-induced thyrotoxicosis occurs most frequently in patients with pre-existing thyroid disease via the Jod–Basedow phenomenon. Patients with autonomously functioning thyroid adenoma(s), previously treated Graves' disease, and colloid goiter are most susceptible. Scintigraphy usually reveals a pattern of MNG, and RAIU is diminished. On the other hand, the patient with iatrogenic or factitious hyperthyroidism will exhibit only background activity on thyroid

scintigraphy and may not have a palpable goiter. RAIU will be very low (Peter F, 2005) .

2.2.6. Mediastinal Goiter

The most common neoplasms of the anterior mediastinum are thymomas, lymphomas, and germ cell tumors. Although retrosternal thyroid accounts for only 7–10% of all mediastinal masses, the non-invasive demonstration of radioiodine uptake within a mediastinal mass is useful as it avoids more invasive tissue diagnosis. Retrosternal thyroid tissue is usually the result of inferior extension of a cervical goiter, but may be related to enlargement of ectopic mediastinal thyroid tissue. Continuity between the cervical and intrathoracic components of a mediastinal goiter may consist of only a narrow fibrous band and may not be demonstrable by CT or ultrasound. If goiter is considered, thyroid scintigraphy should be performed prior to CT imaging to avoid interference

Figure 2.10. Mediastinal goiter. An anterior 123I image demonstrates a relatively normal appearing cervical thyroid accompanied by heterogeneous irregular uptake within the superior mediastinum (Peter F, 2005).

by administration of iodinated contrast media, the most common cause offalse negatives. Due to high background activity related to surrounding blood pool activity, 99mTc images are suboptimal and difficult to interpret. Iodine-123 is the radionuclide of choice for imaging retrosternal thyroid masses. 123I scintigraphy yields high-quality images of thoracic goiters, even when uptake is relatively decreased (Figure 2.10). Despite the fact that clinically significant thyroid cancer occurs in only 4% of mediastinal goiters, the majority of patients with significant mediastinal goiters eventually undergo surgical resection . However, 131I treatment, sometimes augmented by administration of recombinant human TSH (rhTSH), can be used to reduce the size of the mass and alleviate tracheal compression in appropriate patients (Peter F, 2005).

2.2.7. Neonatal Hypothyroidism:

Congenital hypothyroidism (CHT) has an incidence of 1 per 2500–5000 births, and most infants do not exhibit signs or symptoms of hypothyroidism at birth. A delay in the institutionof thyroxine replacement therapy beyond 6–8 weeks of life is likely to be associated with measurable impairment of intellectual function (cretinism). Since the institution of newborn screening programs for CHT by measuring serum TSH and/or T4 levels, the intellectual impairment of CHT has been eradicated in developed countries.

Thyroid dysgenesis (agenesis, hypoplasia, ectopia) is the most common cause of neonatal hypothyroidism in the industrialized world and USA. 99mTc pertechnetate thyroid scintigraphy is performed immediately after CHT is confirmed. It can easily detect eutopic and ectopic thyroid tissue as well as assess degree of thyroidal uptake . Using a pinhole collimator, a close-up and a more distant view (to include the face and chest) in the anterior projection as well as a

lateral view are acquired 20–30 minutes after intravenous injection of 18 MBq (0.5 mCi). A normal image is seen in cases of false positive screening results. A small focus of relatively faint uptake cephalad to the thyroid cartilage is consistent with ectopia and indicates the need for lifelong thyroxine therapy (Figure 2.5). A eutopic enlarged gland with increased uptake, usually marked, is most consistent with dyshormonogenesis; a small proportion of these are due to transient immaturity of the iodine organification process and will be normal at reassessment after age 3 years. Non-visualization of the thyroid on scintigraphy is due to agenesis in over 90% of cases, the remainder being due to the presence of maternal transmission of TSH receptor blocking antibodies; these latter patients will be euthyroid at reassessment when these maternal antibodies have cleared.Patientswith a nonvisualized gland or patients with images suggesting dyshormonogenesis are all re-evaluated at age 3–4 years to exclude transient CHT; patients with ectopia are not reassessed. Therefore, thyroid scintigraphy in the neonate is indispensable in the proper diagnostic work-up of congenital hypothyroidism, because it (1) provides amore specific diagnosis, (2) is cost-effective for selecting patients for subsequent reassessment to uncover transient CHT and allow discontinuation of thyroid hormone replacement therapy, and (3) defines dyshormonogenesis, which is familial and requires genetic counseling (Peter F,2005).

2.3. Image Processing in Nuclear Medicine

Nuclear Medicine is the section of science that utilises the properties of radiopharmaceuticals in order to derive clinical information of the human physiology and biochemistry. According to the examination needed for each patient, a radionuclide is attached to a pharmaceutical (tracer) and the whole complex is then delivered to the patient intravenously or by swallowing or even by

inhalation. The radiopharmaceutical follows its physiological pathway and it is concentrated on specific organs and tissues for short periods of time. Then, the patient is positioned under a nuclear medicine equipment which can detect the radiation emitted by the human body resulting in images of the biodistribution of the radiopharmaceutical.

In Nuclear Medicine, there are two main methods of patient imaging, the imaging with Planar Imaging, Dynamic Imaging or SPECT and the PET. During the last decade, hybrid systems have been developed integrating the CT technique with either SPECT or PET resulting in SPECT/CT and PET/CT respectively.

The gamma camera is composed of a collimator, a scintillator crystal usually made of NaI (or CsI), the photomultiplier tubes, the electronic circuits and a computer equipped with the suitable software to depict the nuclear medicine examinations. In planar imaging, the patient, having being delivered with the suitable radiopharmaceutical, is sited under the gamma camera head. The gamma camera head remains stable at a fixed position over the patient for a certain period of time, acquiring counts (disintegrations). These will constitutethe radiopharmaceutical distribution image. The counts measured in a specific planar projection originate from the whole thickness of patient (Wernick & Aarsvold, 2004).

In SPECT, the gamma camera head rotates around the patient remaining at well defined angles and acquiring counts for specific periods of time per angle. What makes SPECT a valuable tool in nuclear medicine is the fact that information in the three dimensions of the patient can be collected in a number of slices with a finite known volume (in voxels). Thus, SPECT technique is used to display the radiopharmaceutical distribution in a single slice removing the contribution from the overlying and underlying tissues.

In order to obtain the most accurate quantitative data from SPECT images, two issues that have to be resolved are the attenuation correction and the Compton scattering that the photons are undergone until reach and interact with the slice of interest tissues. As an examining organ has certain dimensions, each slice along the axis of the gamma camera has different distance from the detector. Thus, each photon experiences different attenuation. These two phenomena usually lead to distortion of the measured activity concentration (Wernick & Aarsvold, 2004). The acquired data are processed in order to correct and compensate the undesired effect of these physical phenomena. The projection data of each slice constitute the sinogram. As a result, a series of sinograms is the files acquired. However, this kind of files needs reconstruction in order to get an image with diagnostic value. The most known reconstruction methods are the Filtered Back-Projection (FBP) and the Iterative methods.

Attenuation correction is resolved by using the constant linear attenuation coefficient (μ) method or using the transmission source method. In the first one, the distance that each photon has travelled is calculated based on the patient geometry and the exponential reduction of their intensity. Then, considering the human body as a uniform object, an attenuation map is implemented in the reconstructed image. The latter method utilises a transmission source which scans the patient. This depicts each pixel or voxel of the patient with a specific μ producing an attenuation coefficient map. Finally, the attenuation map is implemented on the image resulting in a more accurate diagnosis.

The second issue of scatter correction can be resolved by the electronics of the gamma camera and the filtering process during reconstruction. When a photon undergoes scattering, its energy reduces. So, a well defined function can accept for imaging photons with energy at a certain narrow energy window around the central photopeak of the γ-emission.

A hybrid SPECT/CT scanner is capable of implementing both a CT scan and a SPECT scan or it can be used for each of these scans separately. Using the CT scan, the anatomy of a specific patient area can be imaged while the SPECT scan can depict the physiology of this area. Then, the registration of the two images drives at an image of advanced diagnostic value. Moreover, the CT data is used for the implementation of attenuation correction. (Delbeke , 2006)

The range of nuclear medicine examinations is fairly wide. It includes, among others, patients' studies, as myocardium perfusion by 99mTc-Tetrofosmin or 99mTc-Sestamibi, striatum imaging in brain by 123I-Ioflupane (DaTSCAN), renal parenchyma imaging by 99mTc-De-Methylo-Sulfo-Acid (DMSA) and 99mTc-Methylo-Di-Phosphonate (MDP) for bone scintigraphy. Fundamental image analysis methods of myocardium, brain, kidneys, thyroid, lungs and oncological (e.g. neuroblastoma) nuclear medicine studies include regions' properties, boundary analysis, curvature analysis or line and circle detection.

Image processing serves in reconstruction of images acquired using SPECT techniques, in improvement of the quality of images for viewing and in preparation of images for quantitative results.

Data of the mentioned examinations are used in the following applications of MatLab algorithms to make the image processing and analysis in nuclear medicine clear and show the MatLab utility for these studies.

2.3.1. Image quality in nuclear medicine

Image quality plays an important role in nuclear medicine imaging as the goal is a reliable image of the projected organ to be provided, for accurate diagnosis or therapy. The physical characteristics that are used to describe image quality are (1) contrast, (2) spatial resolution and (3) noise.

Image contrast is the difference in intensity corresponding to different concentration of activity in the patient. For high diagnostic accuracy, nuclear

medicine images must be of high contrast. The image contrast is principally affected by the radiopharmaceutical that is used for imaging and the scattered radiation. In general, it is desirable to use a radiopharmaceutical which has a high uptake within the target organ.

Spatial resolution is defined as the ability of the imaging modality to reproduce the details of a nonuniform radioactive distribution. The spatial resolution is separated into intrinsic resolution (scintillator, photomultiplier tubes and electronic circuit) and system resolution (collimator, scintillator, photomultiplier tubes and electronic circuit). The intrinsic resolution depends on the thickness of scintillation crystal while the system resolution depends mainly on the distance from the emitting source to collimator. The resolution of a gamma camera is limited by several factors. Some of these are the patient motion, the statistical fluctuation in the distribution of visible photons detected and the collimators geometry (Wernick & Aarsvold, 2004).

Noise refers to any unwanted information that prevents the accurate imaging of an object. Noise is the major factor in the degradation of image quality. Image noise may be divided into random and structured noise. Random noise (also referred as statistical noise) is the result of statistical variations in the counts being detected. The image noise is proportional to $N^{1/2}$ where N is the number of detected photons per pixel. Therefore, as the number of counts increases the noise level reduces. Image noise is usually analysed in terms of signal-to-noise-ratio (SNR). SNR is equal to $N/N^{1/2}$. If the SNR is high, the diagnostic information of an image is appreciated regardless of the noise level. Structured noise is derived from non-uniformities in the scintillation camera and overlying structures in patient body.

2.3.2. Image analysis and processing in nuclear medicine:

In the last several decades, medical imaging systems have advanced in a dynamic progress. There have been substantial improvements in characteristics such as sensitivity, resolution, and acquisition speed. New techniques have been introduced and, more specifically, analogue images have been substituted by digital ones. As a result, issues related to the digital images' quality have emerged.

The quality of acquired images is degraded by both physical factors, such as Compton scattering and photon attenuation, and system parameters, such as intrinsic and extrinsic spatial resolution of the gamma camera system. These factors result in blurred and noisy images. Most times, the blurred images present artefacts that may lead to a fault diagnosis. In order the images to gain a diagnostic value for the physician, it is compulsory to follow a specific series of processing.

Image processing is a set of techniques in which the data from an image are analysed and processed using algorithms and tools to enhance certain image information that is more useful to human interpretation (Nailon, 2010). The processing of an image permits theextraction of useful parameters and increases the possibility of detection of small lesions more accurately.

Image processing in nuclear medicine serves three major purposes: a) the reconstruction of the images acquired with tomographic (SPECT) techniques, b) the quality improvement of the image for viewing in terms of contrast, uniformity and spatial resolution and, c) the preparation of the image in order to extract useful diagnostic qualitative and quantitative information.

2.3.3. Digital images

In all modern nuclear medicine imaging systems, the images are displayed as an array ofdiscrete picture elements (pixels) in two dimensions (2D) and are referred as digital images.Each pixel in a digital image has an intensity value and a location

address (Fig. 2.11). In anuclear medicine image the pixel value shows the number of counts recorded in it. The benefit of a digital image compared to the analogue one is that data from a digital image are available for further computer processing.
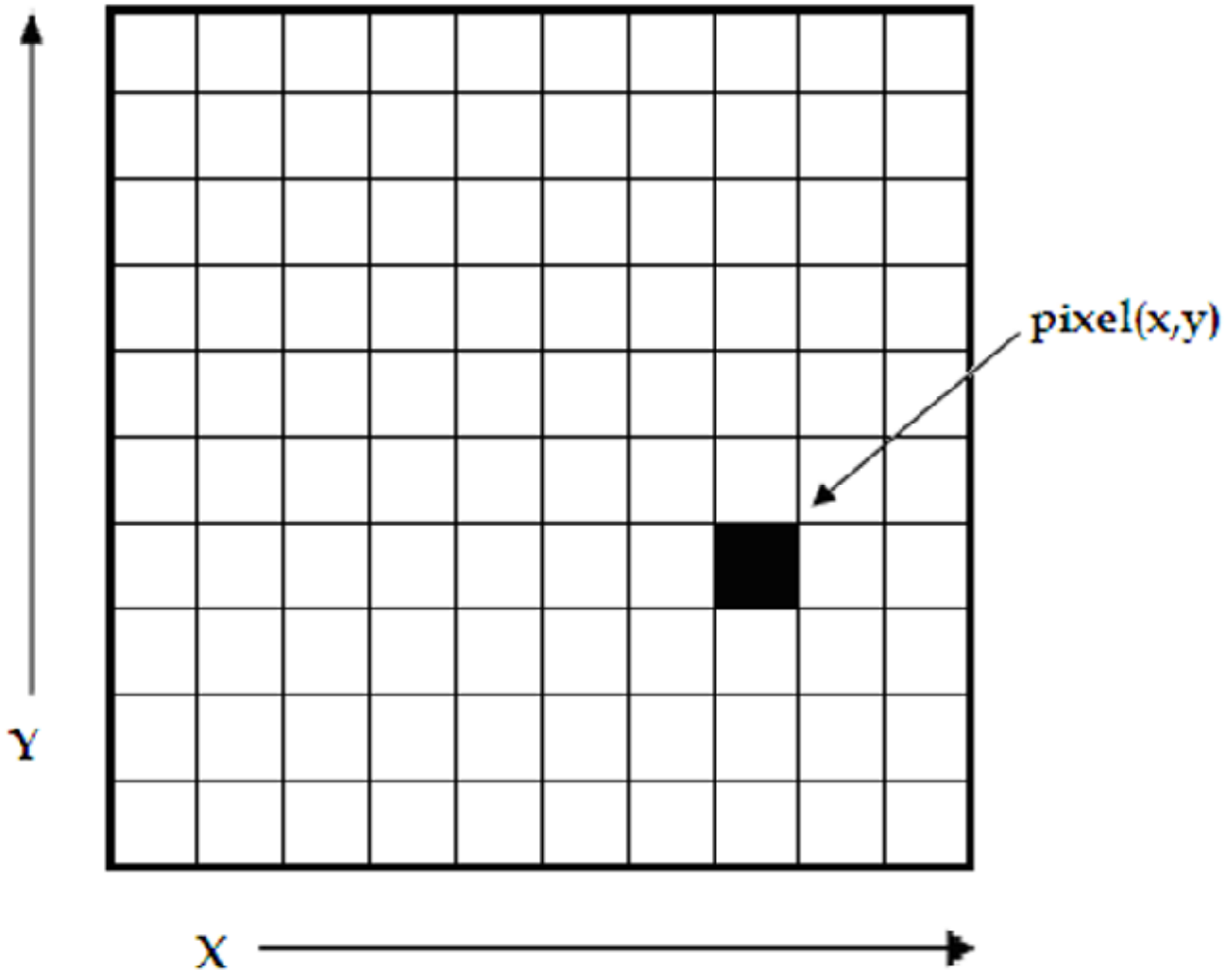
Fig. 2.11. A digital image is a 2D array of pixels. Each pixel is characterised by its (x, y) coordinates and its value.

Digital images are characterised by matrix size, pixel depth and resolution. The matrix size is determined from the number of the columns (m) and the number of rows (n) of the image matrix (m×n). The size of a matrix is selected by the operator. Generally, as the matrix dimension increases the resolution is getting

better (Gonzalez , 2009). Nuclear medicine images matrices are, nowadays, ranged from 64×64 to 1024×1024 pixels.

Pixel or bit depth refers to the number of bits per pixel that represent the colour levels of each pixel in an image. Each pixel can take 2k different values, where k is the bit depth of the image. This means that for an 8-bit image, each pixel can have from 1 to 28 (=256) different color levels (grey-scale levels). Nuclear medicine images are frequently represented as 8- or 16- bit images.

The term resolution of the image refers to the number of pixels per unit length of the image. In digital images the spatial resolution depends on pixel size. The pixel size is calculated by the Field of View (FoV) divided by the number of pixels across the matrix. For a standard FoV, an increase of the matrix size decreases the pixel size and the ability to see details is improved.

2.3.4. Types of digital images – MatLab

MatLab offers simple functions that can read images of many file formats and supports a number of colour maps. Depending on file type and colour space, the returned matrix is either a 2D matrix of intensity values (greyscale images) or a 3D matrix of RGB values. Nuclear medicine images are grey scale or true color images (RGB that is Red, Green and Blue).

The image types supported from the Image Processing Toolbox are listed below:

- Binary Images. In these, pixels can only take 0 or 1 value, black or white.
- Grey scale or intensity images. The image data in a grey scale image represent intensity or brightness. The integers' value is within the range of [0… 2k-1], where k is the bit depth of the image. For a typical grey scale image each pixel can represented by 8 bits and intensity values are in the range of [0…255], where 0 corresponds to black and 255 to white.

- True color or RGB. In these, an image can be displayed using three matrices, each one corresponding to each of red-green-blue color. If in an RGB image each component uses 8 bits, then the total number of bits required for each pixel is 3×8=24 and the range of each individual color component is [0…255].

- Indexed images. Indexed images consist of a 2D matrix together with an m×3 color map (m= the number of the columns in image matrix). Each row of map specifies the red, green, and blue components of a single colour. An indexed image uses direct mapping of pixel values to colour map values. The colour of each image pixel is determined by using the corresponding value of matrix as an index into map.

The greyscale image is the most convenient and preferable type utilised in nuclear medicine image processing. When colouring depiction is needed, the RGB one should be used and processed. The indexed type images should be converted to any of the two other types in order to be processed. The functions used for image type conversion are: rgb2gray, ind2rgb, ind2gray and reversely. Any image can be also transformed to binary one using the command: im2bw. Moreover, in any image, the function impixelinfo can be used in order to detect any pixel value. The user can move the mouse cursor inside the image and the down left corner appears the pixel identity (x, y) as well as the (RGB) values. The pixel range of the image can be displayed by the command imdisplayrange.

2.4. Matlab simulation and programming in thyroid MatLab image tool:

The Image Tool is a simple and user-friendly toolkit which can contribute to a quick image processing and analysis without writing a code and use MatLab

language. These properties makes it a very useful tool when deep analysis is not the ultimate goal but quick processing for better view is desirable.

The Image Tool opens by simply writing the command imtool in the main function window. Then a new window opens and the next step is loading an image. In the menu, there are many functions already installed in order to use it as simple image processing software. The tools include image information appearance, image zooming in and out, panning, adjustment of the window level and width, adjustment of contrast, cropping, distance measurement, conversion of the image to a pixel matrix and colour map choices (grey scale, bone colour, hot regions among others). These are the most common functions likely to be performed in the initial processing approach. Moreover, the user can make some further manipulations such as 3D rotation to respective 3D images and plotting of pixel data.

2.4.1. Image processing techniques – MatLab:

Image processing techniques include all the possible tools used to change or analyse an image according to individuals' needs. This subchapter presents the most widely performed image processing techniques that are applicable to nuclear medicine images. The examples used are mostly come from nuclear medicine renal studies, as kidneys' planar images and SPECT slices are simple objects to show the application of image processing MatLab tools.

2.4.2. Contrast enhancement

One of the very first image processing issues is the contrast enhancement. The acquired image does not usually present the desired object contrast. The improvement of contrast is absolutely needed as the organ shape, boundaries and internal functionality can be better depicted. In addition, organ delineation can be achieved in many cases without removing the background activity.

The command that implements contrast processing is the imadjust. Using this, the contrast in an image can be enhanced or degraded if needed. Moreover, a very useful result can be the inversion of colours, especially in greyscale images, where an object of interest can be efficiently outlined. The general function that implements contrast enhancement is the following:

J = imadjust(I,[low_in high_in],[low_out high_out],gamma);

while the function for colour inversion is the following:

J = imadjust(I,[0 1],[1 0],gamma); or J = imcomplement(I);

suppose that J, is the new image, I, is the initial image and gamma factor depicts the shape of the curve that describes the relationship between the values of I and J. If the gamma factor is omitted, it is considered to be 1.

2.4.3. Organ contour

In many nuclear medicine images, the organs' boundaries are presented unclear due to low resolution or presence of high percentage of noise.

In order to draw the contour of an organ in a nuclear medicine image, the command imcontour is used. In addition, a variable n defines the number of equally spaced contours required. This variable is strongly related with the intensity of counts. For higher n values, the lines are drawn with smaller spaces in between and depict different streaks of intensity. The type of line contouring can be specified as well. For example, when a contour of 5 level contours, drawn with solid line, is the desirable outcome, the whole function is:

Example 1I = imread('thyroid.jpg');

figure, imshow(I)

J = imcontour(I,5,'-');

Figure, imshow(J)

where J and I stands for the final and the initial image respectively and the symbol ('-') stands for the solid line drawing.

2.4.4. Image interpolation

Interpolation is a topic that has been widely used in image processing. It constitutes of the most common procedure in order to resample an image, to generate a new image based on the pattern of an existing one. Moreover, re-sampling is usually required in medical image processing in order to enhance the image quality or to retrieve lost information after compression of an image (Lehmann , 1999). Interpreting the interpolation process, the user is provided with several options. These options include the resizing of an image according to a defined scaling factor, the choice of the interpolation type and the choice of low-pass filter. The general command that performs image resizing is imresize. However, the way that the whole function has to be written depends heavily on the characteristics of the new image. The size of the image can be defined as a scaling factor of the existing image or by exact number of pixels in rows and columns. Concerning the interpolation types usually used in nuclear medicine, these are the following: a) nearest-neighbour interpolation ('nearest'), where the output pixel obtains the value of the pixel that the point falls within, without considering other pixels, b) bilinear interpolation ('bilinear'), where the output pixel obtains a weighted average value of the nearest 2x2 pixels, c) cubic interpolation ('bicubic'), where the output pixel obtains a weighted average value of the nearest 4x4 pixels (Lehmann , 1999).

When an image has to resize in a new one, with specified scaling factor and method, then the function Implementing that, is the following:

NewImage = imresize(Image, scale, method);

For example, for a given image I, the new image J shrunk twice of the initial one, using the bilinear interpolation method, the function will be:

J = imresize(I, 0.5, 'bilinear');

This way of image resizing contributes to the conversion of image information during any such process, a fact that is valuable in the precision of a measurement. Bilinear interpolation is often used to zoom into a 2D image or for rendering, for display purposes. Apart from the previous methods, the cubic convolution method can be applied to 3D images.

2.4.5. Image filtering:

The factors that degrade the quality of nuclear medicine images result in blurred and noisy images with poor resolution. One of the most important factors that greatly affect the quality of clinical nuclear medicine images is image filtering. Image filtering is a mathematical processing for noise removal and resolution recovery. The goal of the filtering is to compensate for loss of detail in an image while reducing noise. Filters suppressed noise as well as deblurred and sharpened the image. In this way, filters can greatly improve the image resolution and limit the degradation of the image.

An image can be filtered either in the frequency or in the spatial domain. In the first case the initial data is Fourier transformed, multiplied with the appropriate filter and then taking the inverse Fourier transform, re-transformed into the spatial domain. The basics steps of filtering in the frequency domain are illustrated in Fig. 2.12.
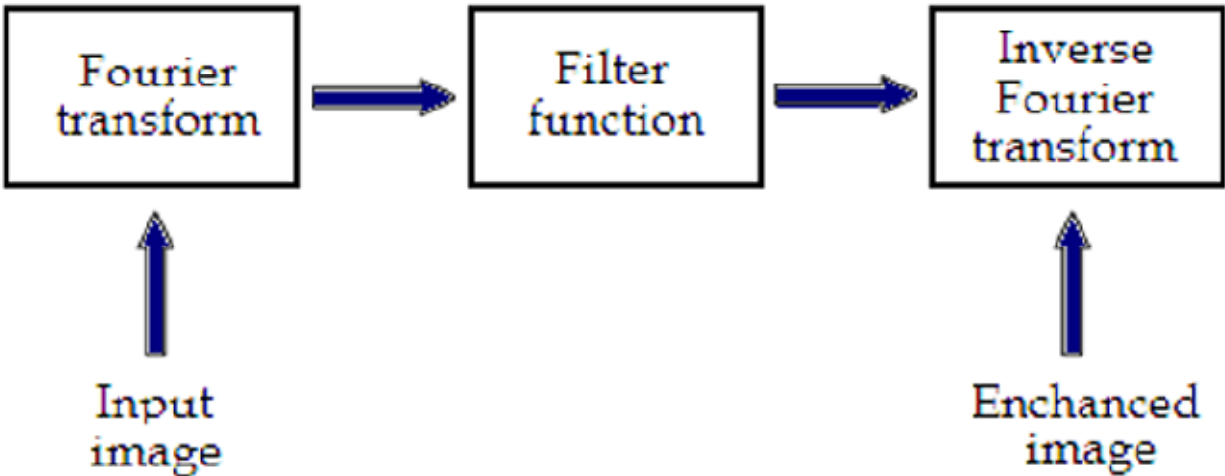
Fig. 12. Basics steps of frequency domain filtering.

The filtering in the spatial domain demands a filter mask (it is also referred as kernel or convolution filter). The filter mask is a matrix of odd usually size which is applied directly on the original data of the image. The mask is centred on each pixel of the initial image. For each position of the mask the pixel values of the image is multiplied by the corresponding values of the mask. The products of these multiplications are then added and the value of the central pixel of the original image is replaced by the sum. This must be repeated for every pixel in the image. The procedure is described schematically in Fig 2.13.

If the filter, by which the new pixel value was calculated, is a linear function of the entire pixel values in the filter mask (e.g. the sum of products), then the filter is called linear. If the output pixel is not a linear weighted combination of the input pixel of the image then the filtered is called non-linear.

According to the range of frequencies they allow to pass through filters can be classified as low pass or high pass. Low pass filters allow the low frequencies to be retained unaltered and block the high frequencies. Low pass filtering removes noise and smooth the image but at the same time blur the image as it does not preserve the edges. High pass filters sharpness the edges of the image (areas in an

image where the signal changes rapidly) and enhance object edge information. A severe disadvantage of high pass filtering is the amplification of statistical noise present in the measured counts.
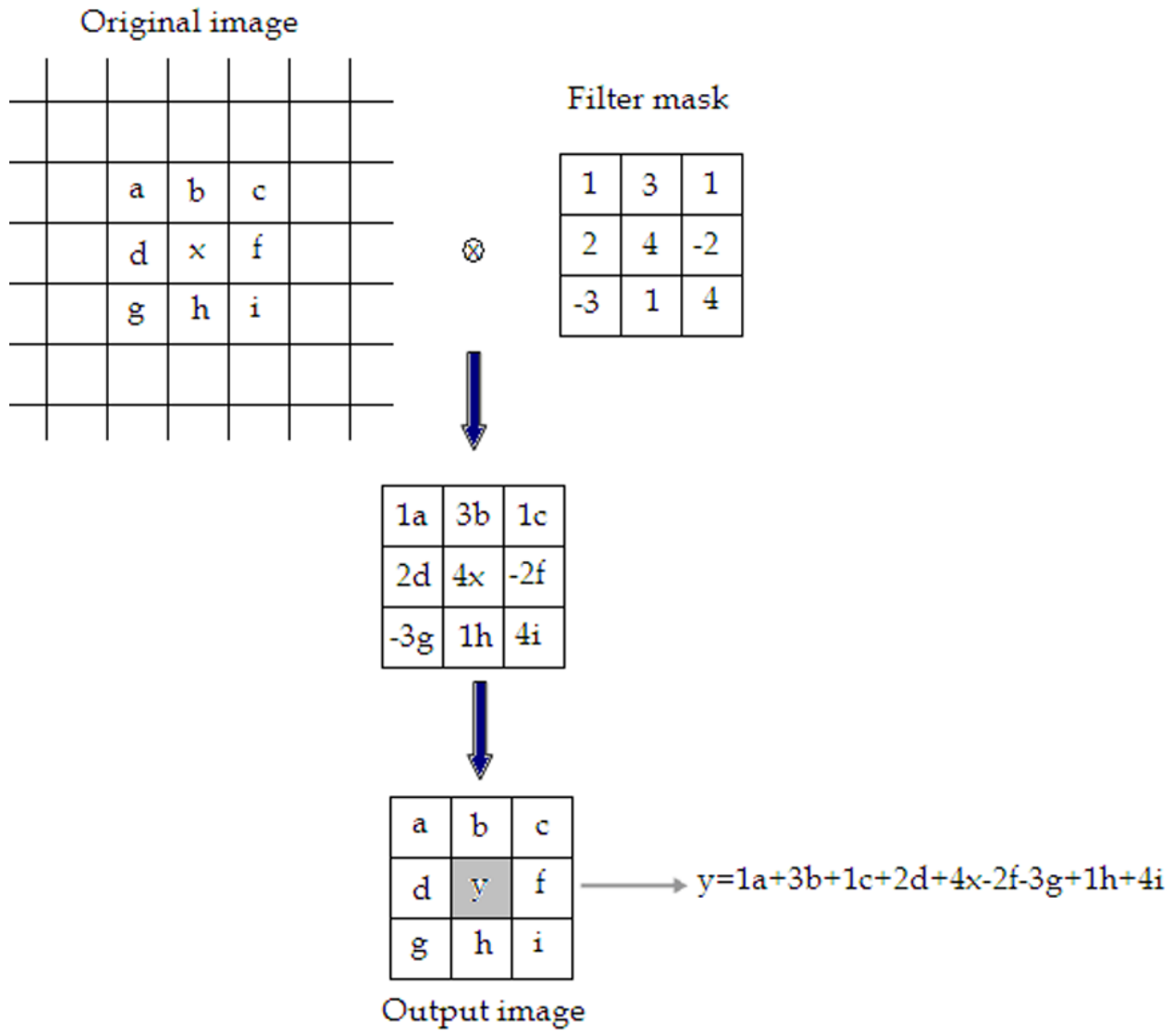
Fig. 2.13. Illustration of filtering process in spatial domain.

2.4.6. Filtering in MatLab

In MatLab, using Image Processing Toolbox we can design and implemented filters for image data. For linear filtering, MatLab provides the fspecial command to generate some predefined common 2D filters.

h=fspecial(filtername, parameters)

The filtername is one of the average, disk, gaussian, laplacian, log, motion, prewitt, sobel and unsharp filters; that is the parameters related to the specific filters that are used each time. Filters are applied to 2D images using the function filter2 with the syntax:

Y = filter2(h,X)

The function filter2 filters the data in matrix X with the filter h. For multidimensional images the function imfilter is used.

B = imfilter(A,h)

This function filters the multidimensional array A with the multidimensional filter h.imfilter function is more general than filter2 function. For nonlinear filtering in MatLab the function nlfilter is applied, requiring three arguments: the input image, the size of the filter and the function to be used.

B = nlfilter(A, [m n], fun)

Example

The following example describes the commands' package that can be used for the application of the mean (average) filter in a SPECT slice for different convolution kernel sizes (for 3×3, 9×9, 25×25 average filter).

h=fspecial('average', [3 3]);

b=imfilter(a,h);

figure, imshow(b);

i=fspecial('average', [9 9]);

```
c=imfilter(b,h);

figure, imshow(c);

j=fspecial('average', [25 25]);

d=imfilter(c,h);

figure, imshow(d);
```

In reviewing of literature in locally and internationally there are some published studies regarding the atuomatic removal of background by many researchers Jianguo et al,(2002) studied A novel method to automatically recognize and remove background signals in computed radiography (CR) images caused by X-ray collimation during projection radiographic examinations is presented. There are three major steps in this method. In the first step, a statistical curve is derived based on many hierarchical CR sample images as a first approximation to loosely separate image and background pixels. Second, signal processing methods, including specific sampling, filtering, and angle recognition, are used to determine edges between image and background pixels. Third, adaptive parameter adjustments and consistent and reliable estimation rules are used to finalize the location of edges and remove the background. In addition, this step also evaluates the reliability of the complete background removal operation. With this novel method implemented in a clinical picture archiving and communication system (PACS) at the University of California at San Francisco, the authors achieved 99% correct recognition of CR image background, and 91% full background removal without removing any valid image information.

Atkins,M.S et al, (2002) studied A robust fully automatic method for segmenting the brain from head magnetic resonance (MR) images has been developed, which works even in the presence of radio frequency (RF) inhomogeneities. It has been successful in segmenting the brain in every slice from head images acquired from

several different MRI scanners, using different-resolution images and different echo sequences. The method uses an integrated approach which employs image processing techniques based on anisotropic filters and "snakes" contouring techniques, and a priori knowledge, which is used to remove the eyes, which are tricky to remove based on image intensity alone. It is a multistage process, involving first removal of the background noise leaving a head mask, then finding a rough outline of the brain, then refinement of the rough brain outline to a final mask. The paper describes the main features of the method, and gives results for some brain studies.

Chenyu Wu et al ,(2004) studied an intelligent image editing and face synthesis system that automatically removes eyeglasses from an input frontal face image. Although conventional image editing tools can be used to remove eyeglasses by pixel-level editing, filling in the deleted eyeglasses region with the right content is a difficult problem. Our approach works at the object level where the eyeglasses are automatically located, removed as one piece, and the void region filled. Our system consists of three parts: eyeglasses detection, eyeglasses localization, and eyeglasses removal. First, an eye region detector, trained offline, is used to approximately locate the region of eyes, thus the region of eyeglasses. A Markov-chain Monte Carlo method is then used to accurately locate key points on the eyeglasses frame by searching for the global optimum of the posterior. Subsequently, a novel sample-based approach is used to synthesize the face image without the eyeglasses. Specifically, we adopt a statistical analysis and synthesis approach to learn the mapping between pairs of face images with and without eyeglasses from a database. Extensive experiments demonstrate that our system effectively removes eyeglasses.

Chapter Three
Materials and Methods

3.1. Material:

The two images that were used in this study taken by scintillation gamma camera.

3.2. Methods:

3.2.1 Study duration:

This study performed in period between September 2014 and February 2015.

3.2.2. Study place:

This study carried out In Al Nelein Diagnostic Center.

3.2.3. Sampling:

Two patients undergoing thyroid imaging in the Nuclear Medicine department In Al Nelein Diagnostic Center.

3.2.4. Methods of data Collection:

A thyroid gland scintography can be easily detected in an image if the object has sufficient contrast from the background. Edge detection and basic morphology tools were used to detect a thyroid gland.

3.2.4.1. Steps of segmentation technique:

The six steps of segmentation technique are described in the follow chart bellow
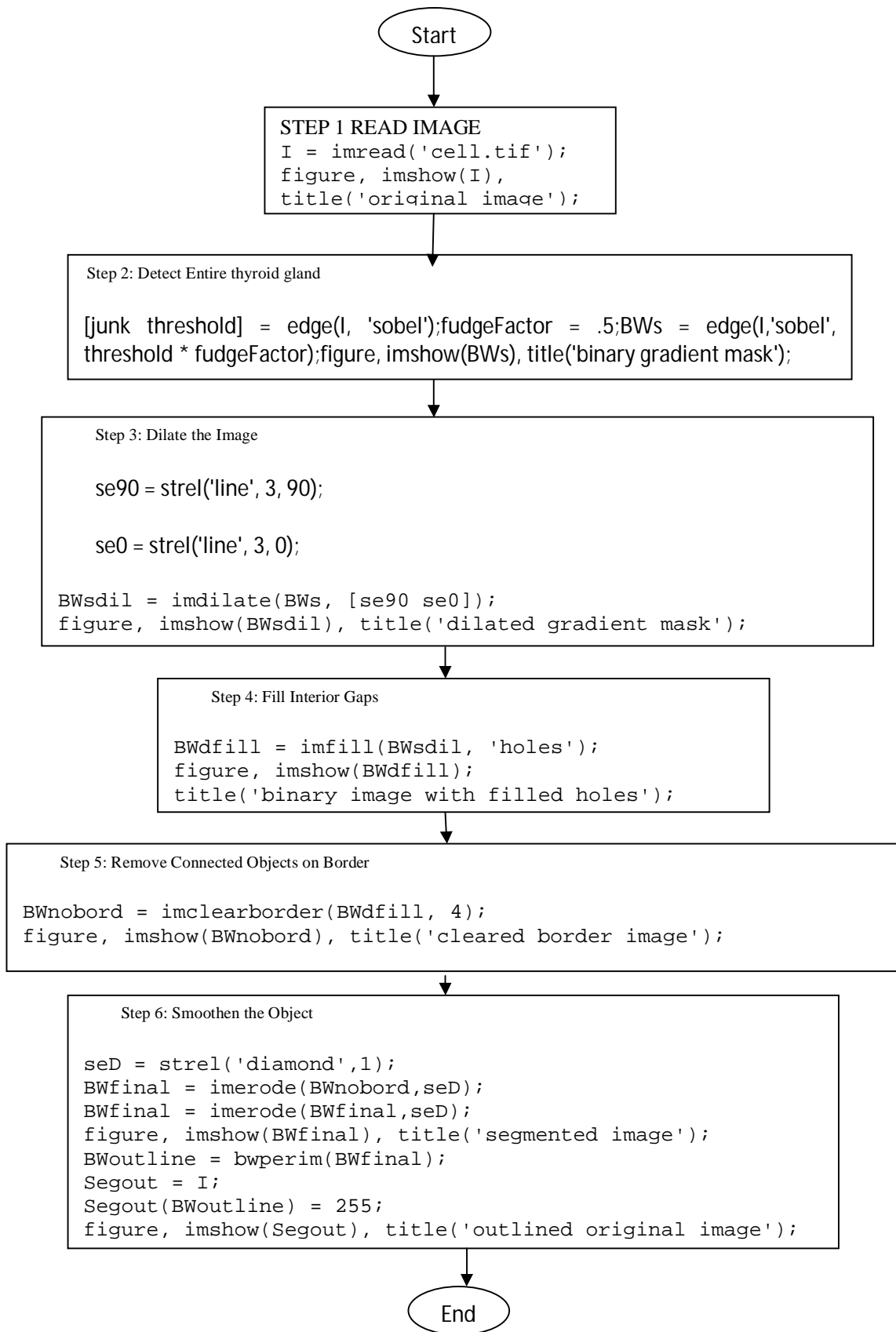
```
                        ( Start )
                            │
                            ▼
┌───────────────────────────────────────┐
│ STEP 1 READ IMAGE                      │
│ I = imread('cell.tif');                │
│ figure, imshow(I),                     │
│ title('original image');               │
└───────────────────────────────────────┘
                            │
                            ▼
┌─────────────────────────────────────────────────────────────┐
│ Step 2: Detect Entire thyroid gland                          │
│                                                              │
│ [junk threshold] = edge(I, 'sobel');fudgeFactor = .5;BWs =   │
│ edge(I,'sobel', threshold * fudgeFactor);figure, imshow(BWs),│
│ title('binary gradient mask');                               │
└─────────────────────────────────────────────────────────────┘
                            │
                            ▼
┌─────────────────────────────────────────────────────────────┐
│ Step 3: Dilate the Image                                     │
│                                                              │
│   se90 = strel('line', 3, 90);                               │
│                                                              │
│   se0 = strel('line', 3, 0);                                 │
│                                                              │
│ BWsdil = imdilate(BWs, [se90 se0]);                          │
│ figure, imshow(BWsdil), title('dilated gradient mask');      │
└─────────────────────────────────────────────────────────────┘
                            │
                            ▼
┌───────────────────────────────────────────────┐
│ Step 4: Fill Interior Gaps                     │
│                                                │
│   BWdfill = imfill(BWsdil, 'holes');           │
│   figure, imshow(BWdfill);                     │
│   title('binary image with filled holes');     │
└───────────────────────────────────────────────┘
                            │
                            ▼
┌─────────────────────────────────────────────────────────────┐
│ Step 5: Remove Connected Objects on Border                   │
│                                                              │
│ BWnobord = imclearborder(BWdfill, 4);                        │
│ figure, imshow(BWnobord), title('cleared border image');     │
└─────────────────────────────────────────────────────────────┘
                            │
                            ▼
┌───────────────────────────────────────────────────────┐
│ Step 6: Smoothen the Object                            │
│                                                        │
│   seD = strel('diamond',1);                            │
│   BWfinal = imerode(BWnobord,seD);                     │
│   BWfinal = imerode(BWfinal,seD);                      │
│   figure, imshow(BWfinal), title('segmented image');   │
│   BWoutline = bwperim(BWfinal);                        │
│   Segout = I;                                          │
│   Segout(BWoutline) = 255;                             │
│   figure, imshow(Segout), title('outlined original    │
│   image');                                             │
└───────────────────────────────────────────────────────┘
                            │
                            ▼
                        ( End )
```

Figure (3-1) shows the segmentation steps

3.2.5. Methods of data analysis:

The thyroid images taken were treated using software MATLAB R2009B.

3.2.6. Method of data storage:

The data stored securely in password personal computer (PC)

3.2.7.Ethical issue:

- Permission from the Nuclear Medicine department In Al Nelein Diagnostic

- No patients' details were disclosed.

Chapter four

The Result

4.1. First image:

Step 1: Read Image:

Step 1: Read Image (figure 3-1)

original image

Figure (4-1) shows the Original thyroid gland image

Step 2: Detect Entire thyroid gland:

Two thyroid gand are present in this image, but only one thyroid can be seen in its entirety. We will detect this thyroid. Another word for object detection is segmentation. The object to be segmented differs greatly in contrast from the background image. Changes in contrast can be detected by operators that calculate the gradient of an image. The gradient image can be calculated and a threshold can be applied to create a binary mask containing the segmented thyroid. First,was use edge and the Sobel operator to calculate the threshold

value. then tune the threshold value and use edge again to obtain a binary mask that contains the segmented thyroid gland.

binary gradient mask

Figure (4-2) shows the Entire thyroid gland

Step 3: Dilate the Image:

The binary gradient mask shows lines of high contrast in the image. These lines do not quite delineate the outline of the object of interest. Compared to the original image, you can see gaps in the lines surrounding the object in the gradient mask. These linear gaps will disappear if the Sobel image is dilated using linear structuring elements, which can create with the strel function.The binary gradient mask is dilated using the vertical structuring element followed by the horizontal structuring element. The imdilate function dilates the image.

dilated gradient mask
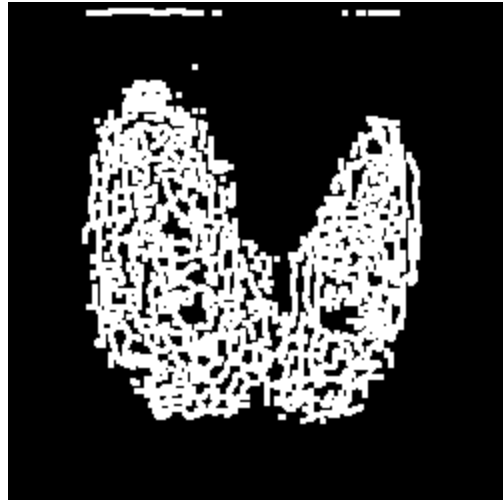
Figure(4-3) shows the Dilated Image

Step 4: Fill Interior Gaps:

The dilated gradient mask shows the outline of the thyroid gland quite nicely, but there are still holes in the interior of the thyroid gland. To fill these holes   the imfill function was used.

binary image with filled holes

Figure (4-4) shows the Filled Interior Gaps image

Step 5: Remove Connected Objects on Border:

The thyroid of interest has been successfully segmented, but it is not the only object that has been found. Any objects that are connected to the border of the image can be removed using the imclearborder function. The connectivity in the imclearborder function was set to 4 to remove diagonal connections.

cleared border image
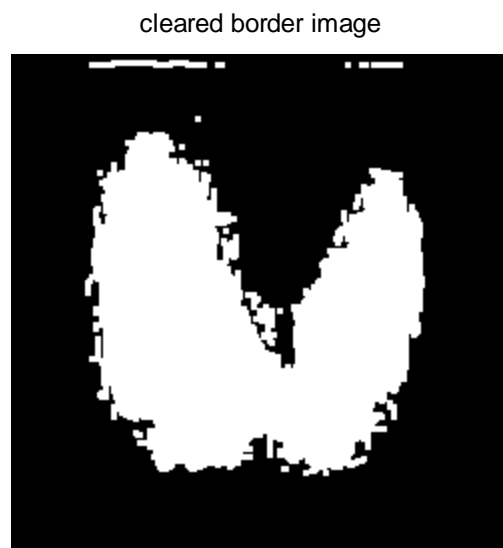
Figure (4-5) shows the clear border image.

Step 6: Smoothen the Object:

Finally, in order to make the segmented object look natural, the object was smoothen by eroding the image twice with a diamond structuring element. create the diamond structuring element using the strel function.

segmented image

Figure (4-6) shows the Smoothen Object image.

An alternate method for displaying the segmented object would be to place an outline around the segmented thyroid.
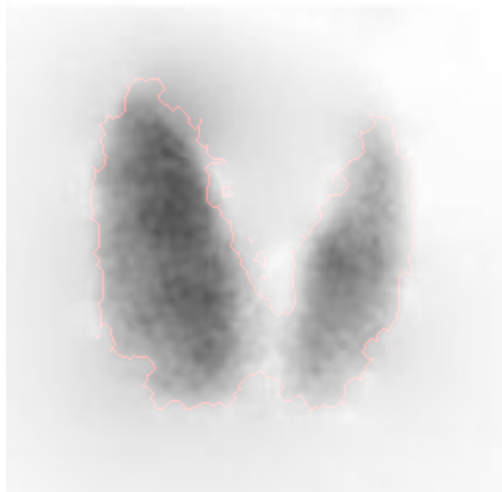

outlined original image

Figure (4-7) shows the outlined original image of thyroid

4. 2. Second image:

Step 1: Read Image:
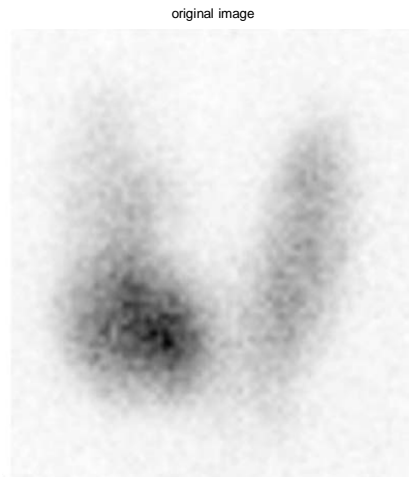
Step 1: Read Image (figure 4-8)

original image

Figure (4-8) shows the Original thyroid gland image.

Step 2: Detect Entire thyroid gland:

Two thyroid gand are present in this image, but only one thyroid can be seen in its entirety. We will detect this thyroid. Another word for object detection is segmentation. The object to be segmented differs greatly in contrast from the background image. Changes in contrast can be detected by operators that calculate the gradient of an image. The gradient image can be calculated and a threshold can be applied to create a binary mask containing the segmented thyroid. First,was use edge and the Sobel operator to calculate the threshold value. then tune the threshold value and use edge again to obtain a binary mask that contains the segmented thyroid gland.
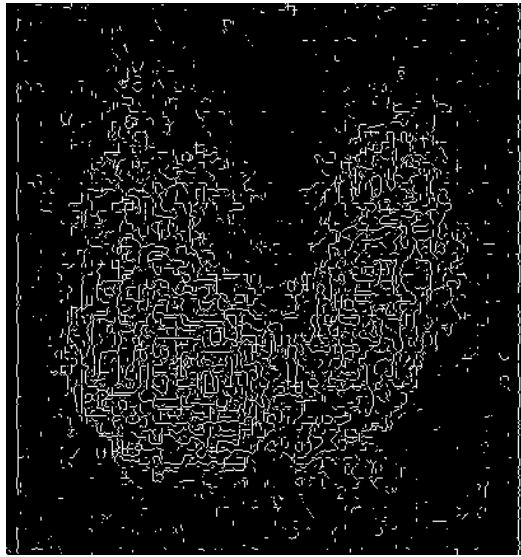
binary gradient mask

Figure (4-9) shows the Entire thyroid gland.

Step 3: Dilate the Image:

The binary gradient mask shows lines of high contrast in the image. These lines do not quite delineate the outline of the object of interest. Compared to the original image, you can see gaps in the lines surrounding the object in the gradient mask. These linear gaps will disappear if the Sobel image is dilated using linear structuring elements, which can create with the strel function.The binary gradient mask is dilated using the vertical structuring element followed by the horizontal structuring element. The imdilate function dilates the image.
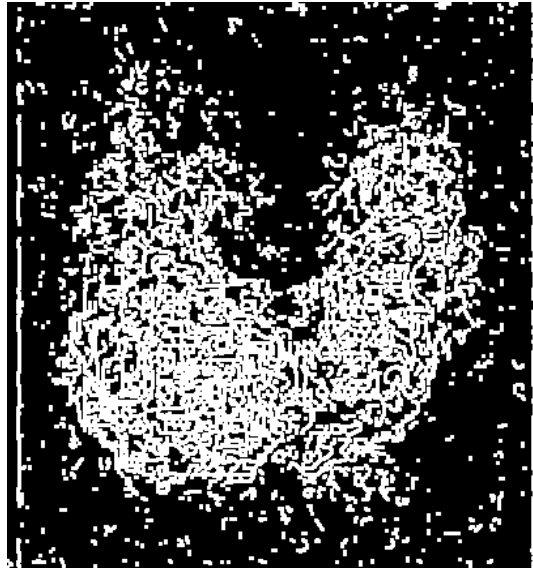
dilated gradient mask

Figure (4-10) shows the Dilated Image.

Step 4: Fill Interior Gaps:

The dilated gradient mask shows the outline of the thyroid gland quite nicely, but there are still holes in the interior of the thyroid gland. To fill these holes   the imfill function was used.

binary image with filled holes

Figure (4-11) shows the Filled Interior Gaps image

Step 5: Remove Connected Objects on Border:

The thyroid of interest has been successfully segmented, but it is not the only object that has been found. Any objects that are connected to the border of the image can be removed using the imclearborder function. The connectivity in the imclearborder function was set to 4 to remove diagonal connections.

cleared border image

Figure (4-12) shows the clear border image

Step 6: Smoothen the Object:

Finally, in order to make the segmented object look natural, the object was smoothen by eroding the image twice with a diamond structuring element. We create the diamond structuring element using the strel function.

segmented image

Figure (4-13) shows the Smoothen Object image.

An alternate method for displaying the segmented object would be to place an outline around the segmented thyroid.
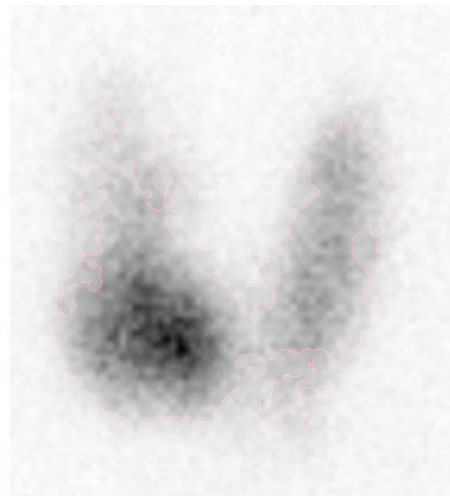

outlined original image

Figure (4-14) shows the outlined original image of thyroid .

Chapter five

Discussion, Conclusion and Recommendations

5.1 Discussion :

The study was aimed to Automatic removal of background of thyroid scintigraphy using image processing technique, the study was done in Alneelain Diagnostic center, Two thyroid images (scintigraphy) were processed using MATLAB R2009b with details as follows: the image readed, The gradient image calculated and a threshold was applied to created a binary mask containing the segmented thyroid. First,was use edge and the Sobel operator to calculate the threshold value. then tune the threshold value and use edge again to obtain a binary mask that contains the segmented thyroid gland.Sobel image was dilated using linear structuring elements, which can create with the strel function.The binary gradient mask is dilated using the vertical structuring element followed by the horizontal structuring element The dilated gradient mask shows the outline of the thyroid gland quite nicely, but there are still holes in the interior of the thyroid gland. To fill these holes the imfill function was used. The thyroid of interest has been successfully segmented, but it is not the only object that has been found. Any objects that are connected to the border of the image can be removed using the imclearborder function, the object was smoothen by eroding the image twice with a diamond structuring element An alternate method for displaying the segmented object was placed an outline around the segmented thyroid. Jianguo et al,(2002) studied A novel method to automatically recognize and remove background signals in computed radiography (CR) images caused by X-ray collimation during projection radiographic examinations is presented. There are three major steps in this method. In the first step, a statistical curve is derived based on many

hierarchical CR sample images as a first approximation to loosely separate image and background pixels. Second, signal processing methods, including specific sampling, filtering, and angle recognition, are used to determine edges between image and background pixels. Third, adaptive parameter adjustments and consistent and reliable estimation rules are used to finalize the location of edges and remove the background. In addition, this step also evaluates the reliability of the complete background removal operation. With this novel method implemented in a clinical picture archiving and communication system (PACS) at the University of California at San Francisco, the authors achieved 99% correct recognition of CR image background, and 91% full background removal without removing any valid image information. Atkins,M.S.et al,(2002) studied A robust fully automatic method for segmenting the brain from head magnetic resonance (MR) images has been developed, which works even in the presence of radio frequency (RF) inhomogeneities. It has been successful in segmenting the brain in every slice from head images acquired from several different MRI scanners, using different-resolution images and different echo sequences. The method uses an integrated approach which employs image processing techniques based on anisotropic filters and "snakes" contouring techniques, and a priori knowledge, which is used to remove the eyes, which are tricky to remove based on image intensity alone. It is a multistage process, involving first removal of the background noise leaving a head mask, then finding a rough outline of the brain, then refinement of the rough brain outline to a final mask. The paper describes the main features of the method, and gives results for some brain studies. Chenyu Wu et al,(2004) studied an intelligent image editing and face synthesis system that automatically removes eyeglasses from an input frontal face image. Although conventional image editing tools can be used to remove eyeglasses by pixel-level editing, filling in the deleted eyeglasses region with the right content is a difficult problem. Our approach works at the

object level where the eyeglasses are automatically located, removed as one piece, and the void region filled. Our system consists of three parts: eyeglasses detection, eyeglasses localization, and eyeglasses removal. First, an eye region detector, trained offline, is used to approximately locate the region of eyes, thus the region of eyeglasses. A Markov-chain Monte Carlo method is then used to accurately locate key points on the eyeglasses frame by searching for the global optimum of the posterior. Subsequently, a novel sample-based approach is used to synthesize the face image without the eyeglasses. Specifically, we adopt a statistical analysis and synthesis approach to learn the mapping between pairs of face images with and without eyeglasses from a database. Extensive experiments demonstrate that our system effectively removes eyeglasses

5.2 Conclusion :

This study was designed to enhancement of edge of thyroid scintigraph using image processing technique. The software is implemented using MATLAB R2009b image segmentation method was applied into two images was taken from Nuclear Medicine department the set of images which are gray scale . the original images in figure (4-1) and figure(4-8) after processing became with outline showen in figure (4-7) and figure (4-14) .

5.3 Recommendations:

The production of two-dimensional images of the distribution of radioactivity in thyroid after the internal administration of radionuclide the images being obtained by a scintillation camera they are sometimes not clear or with unsharpness , blurring and there are problems of false edge detection, missing true edges, edge localization that will lead to difficulties in diagnosis of thyroid cancer or other

disorder need scintigraphy imaging and may be lead to wrong diagnosis, In these case it must implement one of the edge detection oprators to Find edges of objects in images using Sobel, Prewitt, Roberts, or Canny method or technique of removal background.

References:

Alzahrani AS, Bakheet S,Mandil MA, (2001). 123I isotope as a diagnostic agent in the follow-up of patients with differentiated thyroid cancer: Comparison with post 131I therapy whole body scanning. J Clin Endocrinol Metab; 86:5294–5300.

Bankman, I. (2000). *Handbook of Medical Imaging*, Academic Press, ISSN 0-12-077790-8, United States of America

Delbeke, D.; Coleman, R.E.; Guiberteau M.J.; Brown, M.L.; Royal, H.D.; Siegel, B.A.; Townsend, D.W.; Berland, L.L.; Parker, J.A.; Zubal, G. & Cronin, V. (2006). Procedure Guideline for SPECT/CT Imaging 1.0. *The Journal of Nuclear Medicine*, Vol. 47, No. 7, (July 2006), pp. (1227-1234).

Grigsby PW, Siegel BA, Bekker S, 2004, Preparation of patients with thyroid cancer for 131I scintigraphy or therapy by 1–3 weeks of thyroxine discontinuation. J Nucl Med; 45:567–570.

Gonzalez, R.; Woods, R., & Eddins, S. (2009) *Digital Image Processing using MATLAB*, (second edition), Gatesmark Publishing, ISBN 9780982085400, United States of America

Lehmann, T.M.; Gönner, C. & Spitzer, K. (1999). Survey: Interpolation Methods in Medical Image Processing. *IEEE Transactions on Medical Imaging*, Vol.18, No.11, (November 1999), pp. (1049-1075), ISSN S0278-0062(99)10280-5

Nailon, W.H. (2010). Texture Analysis Methods for Medical Image Characterisation, Biomedical Imaging, Youxin Mao (Ed.), ISBN: 978-953-307-071-1, InTech, Available from: http://www.intechopen.com/articles/show/title/texture-analysis-methodsfor-medical-image-characterisation.

O' Gorman, L.; Sammon, M. & Seul M. (2008). *Practicals Algorithms for image analysis*, (second edition), Cambridge University Press, 978-0-521-88411-2, United States of Americ"

Perutka K, 2010, Tips and Tricks for Programming in Matlab, Matlab - Modelling, Programming and Simulations, Emilson Pereira Leite (Ed.), ISBN: 978-953-307-125-1, InTech, Available from: http://www.intechopen.com/articles/show/title/tipsand- tricks-for-programming-in-matlab.

Peter F. Sharp, Howard G. Gemmell and Alison D. Murray (Eds),(2005), Practical Nuclear Medicine.

William D. Leslie and David Greenberg ,2003, Nuclear Medicine , Landes Bioscience ISBN: 1-57059-644-1.